

# Neural Network Potentials to explore the Crystal Structure Landscape

Stefano de Gironcoli

*Scuola Internazionale Superiore di Studi Avanzati  
Trieste-Italy*



## Credits:

Emine Kucukbenli, Boston U (MA, USA)

Ruggero Lot, SISSA Trieste (I)

Franco Pellegrini, SISSA Trieste (I)

Yusuf Shaidu, Berkeley (CA, USA)

## PANNA

Properties from Artificial Neural Network Architectures

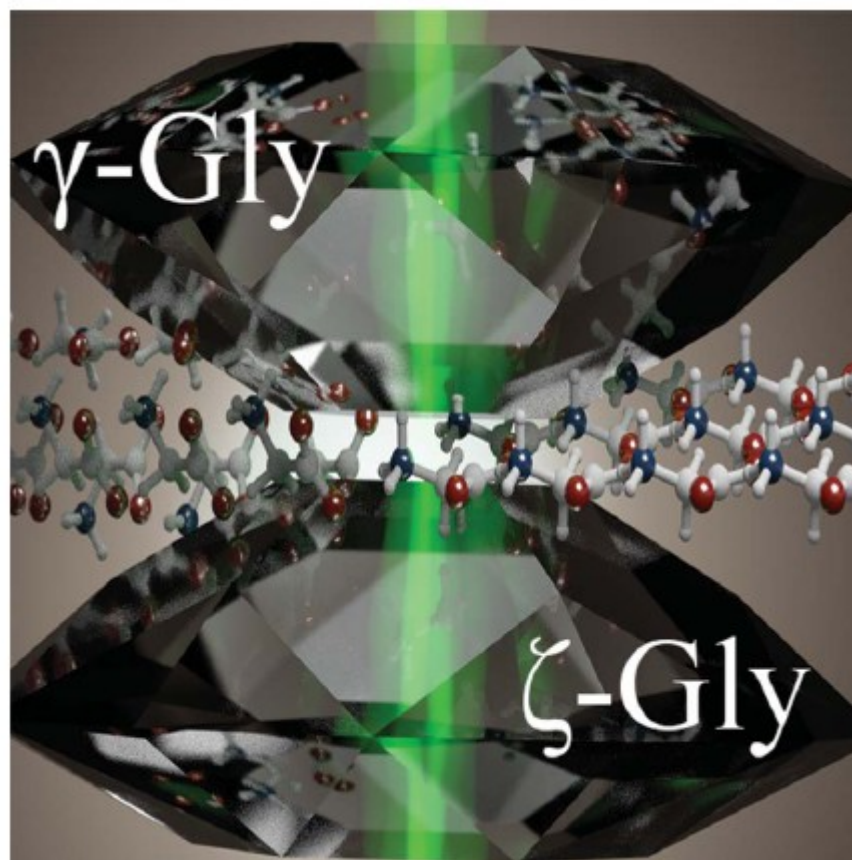
<https://gitlab.com/pannadevs/panna>



# CSP is a formidable task

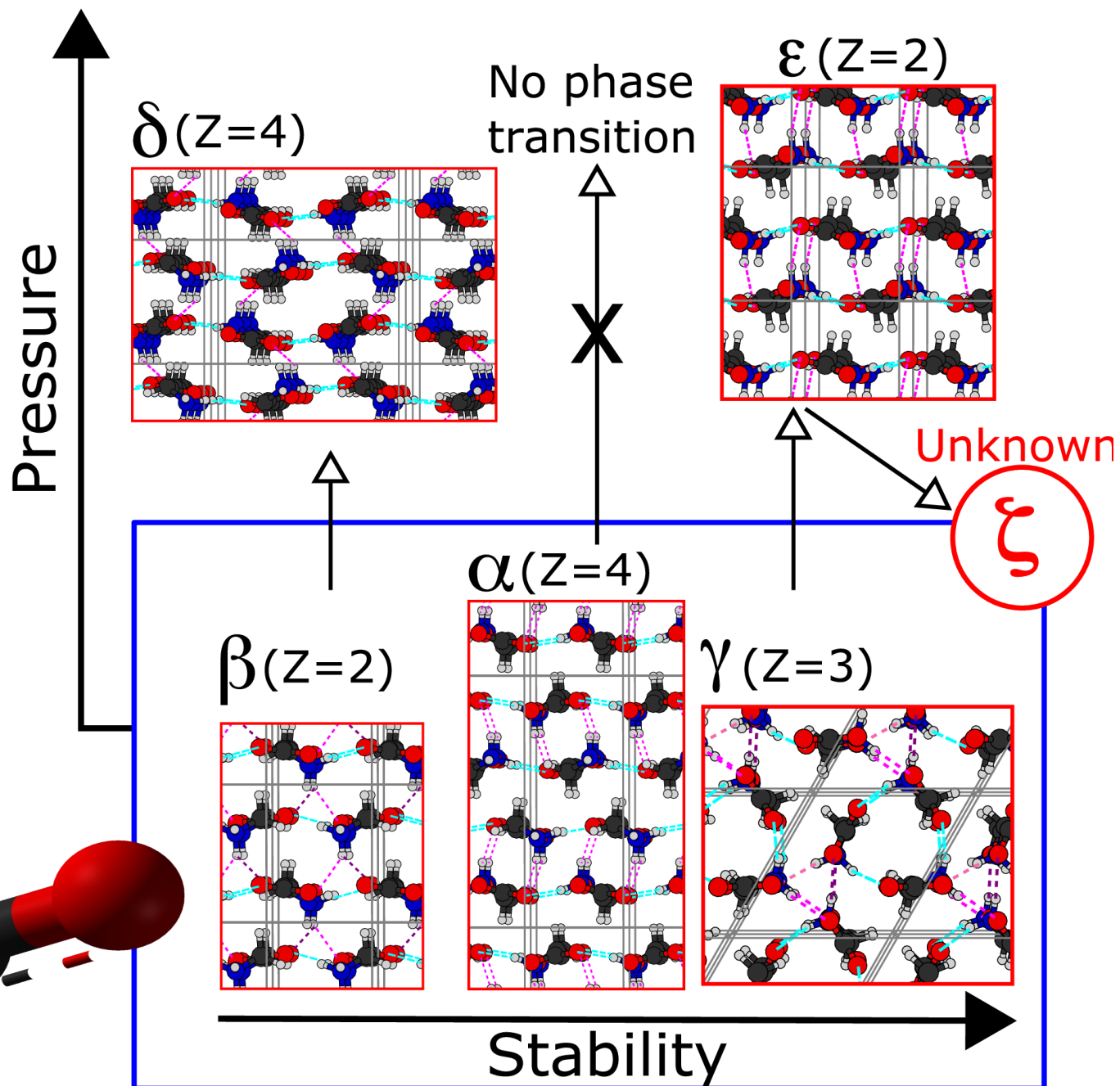
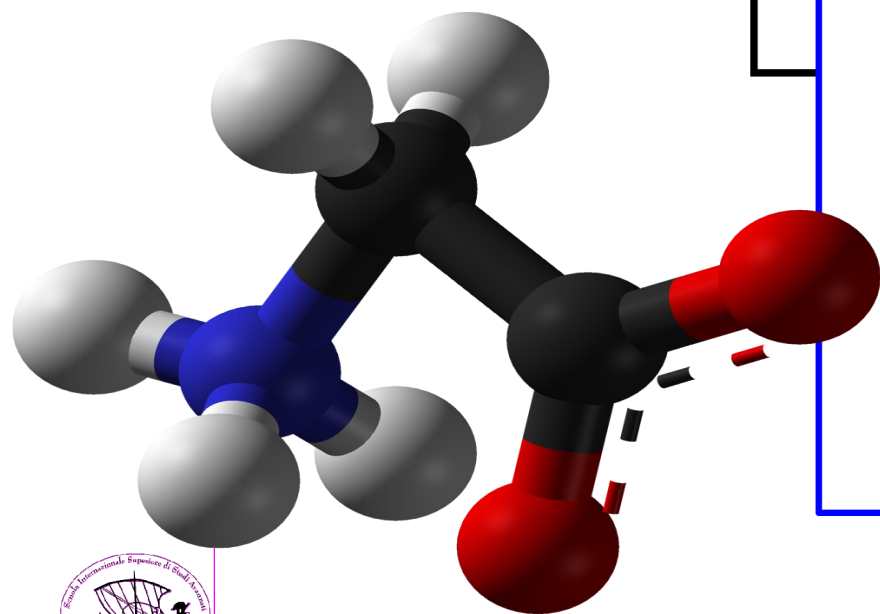
- CSP problem: Name a chemical or stoichiometric formula; find the (local) minima of the free energy landscape under given thermodynamic conditions (often at certain T,P)
- “What is the most stable structure of glycine at ambient conditions?” “What is the carbon structure that is stable at very high pressures”
- Challenges:
  - A very vast space of possibilities.
  - Free energy landscape is very expensive to obtain accurately

# $\zeta$ -Glycine: Insight into the mechanism of a polymorphic phase transition





# Glycine



# How to tackle CSP?

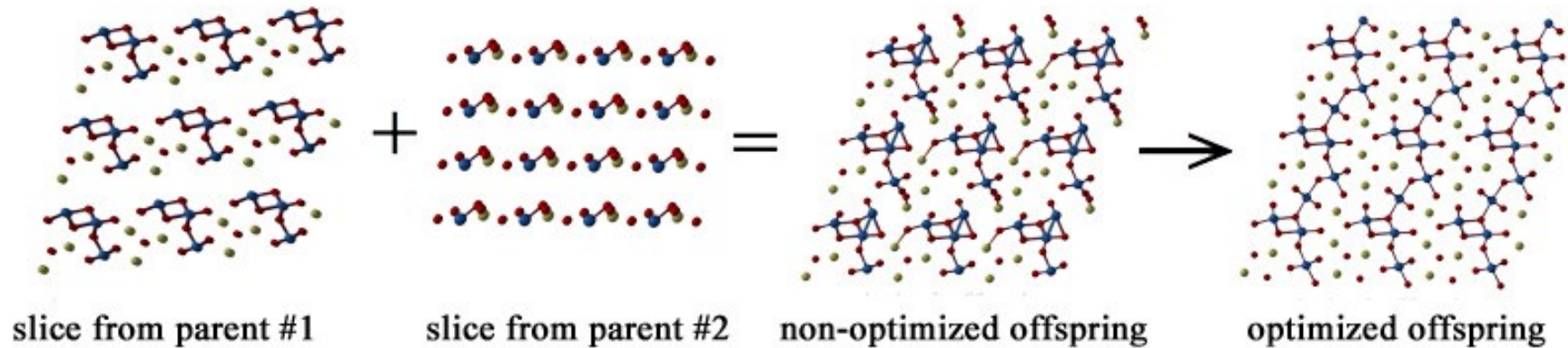
Explore: Use smart algorithms to explore as much of the landscape as possible

Molecular dynamics / Monte Carlo walkers

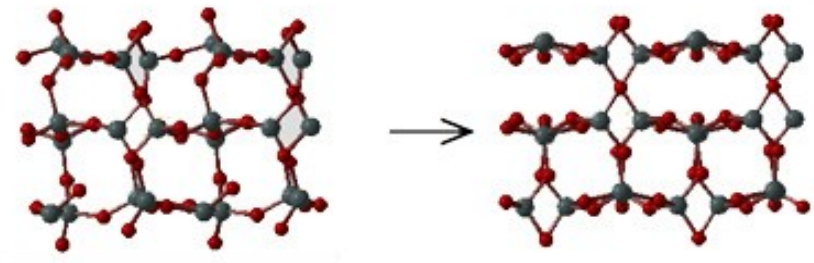
- Simulated annealing
  - Metadynamics
  - Basin hopping
  - Minima hopping
  - Genetic algorithm
-

# Genetic algorithm

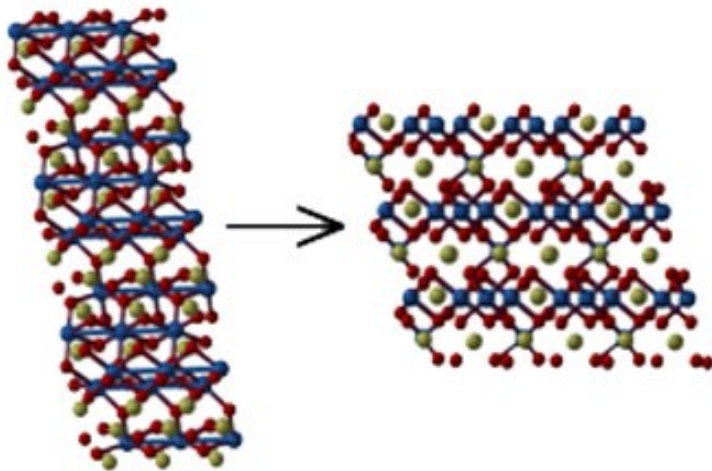
(a) heredity



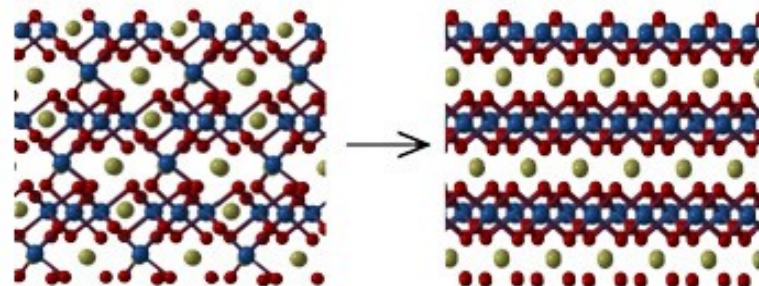
(c) softmode mutation



(b) lattice mutation



(d) permutation



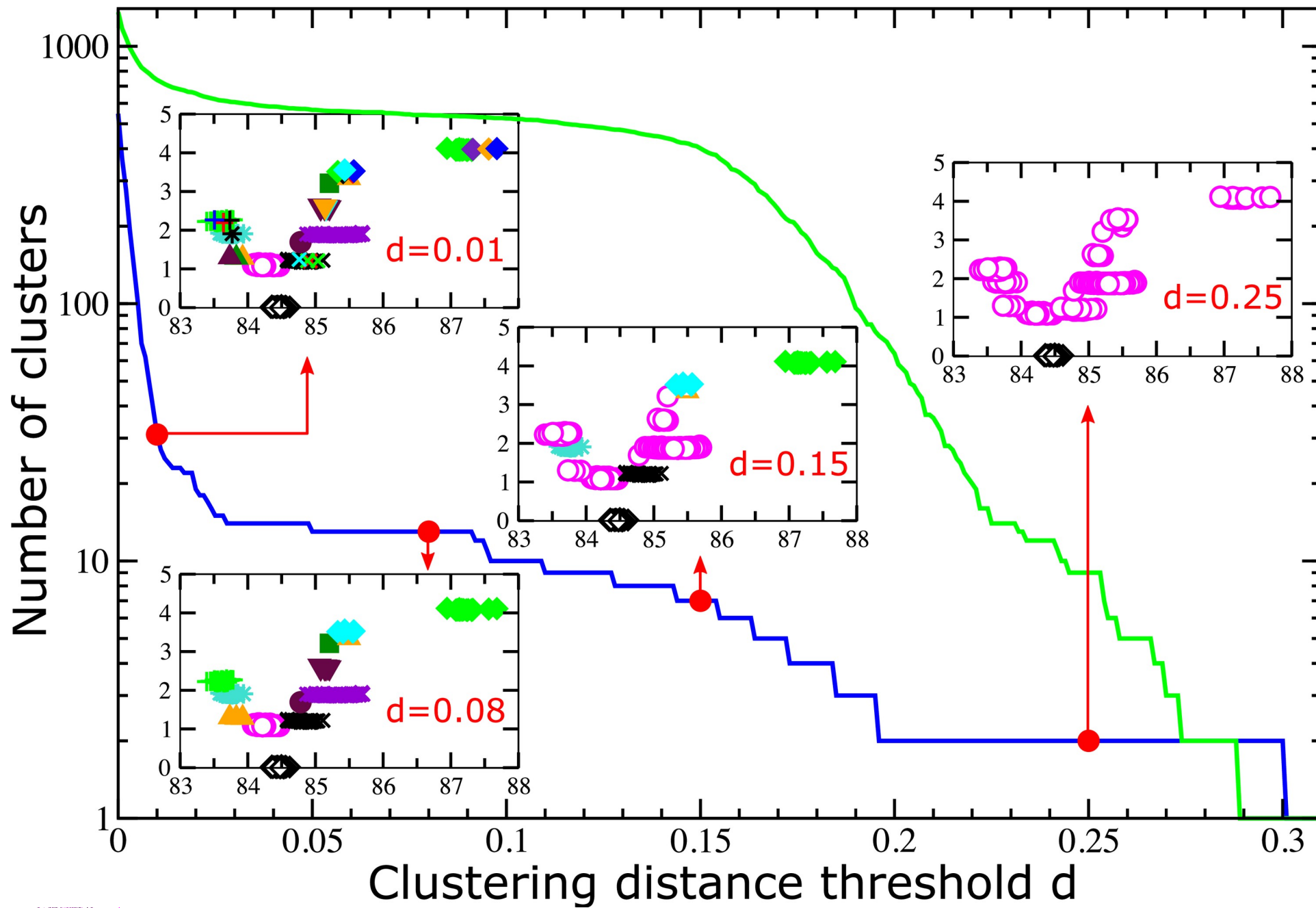
USPEX operations



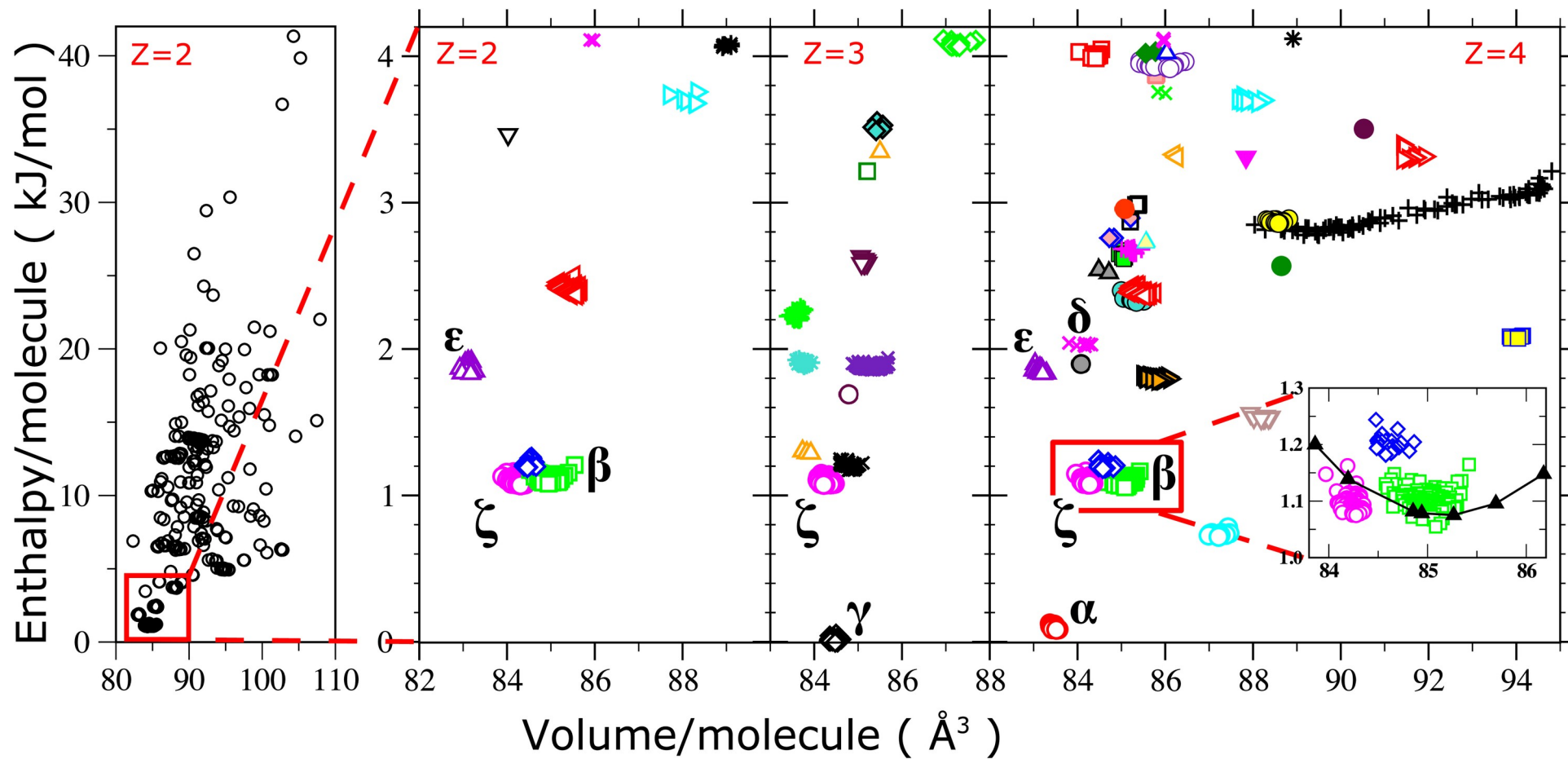
+



+ vdWDF + clustering







# $\zeta$ -phase

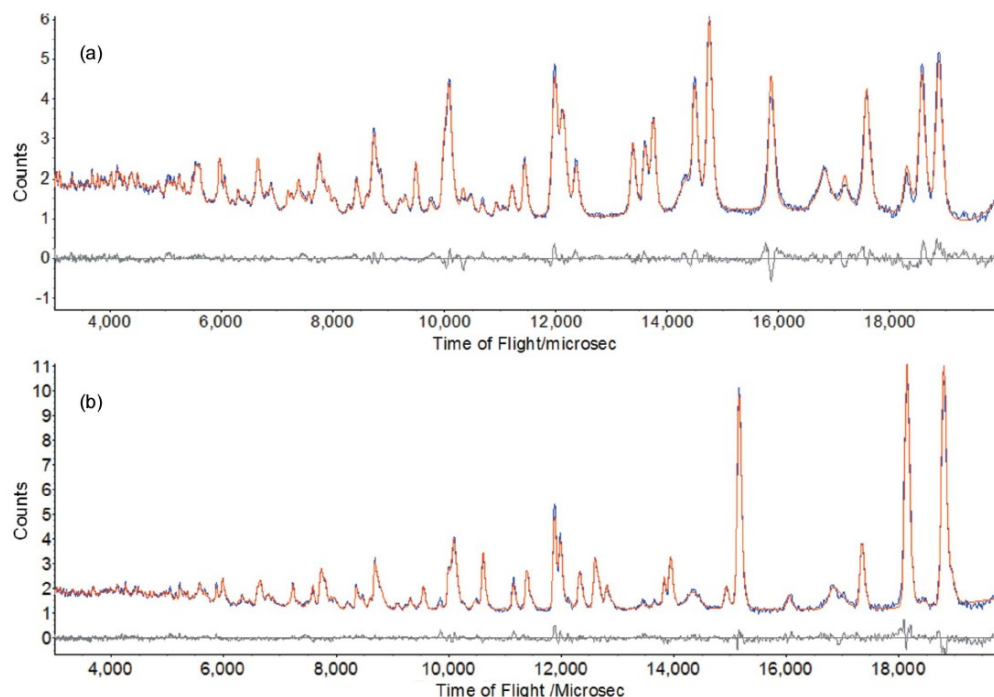


Figure 2

(a) Rietveld fit of the neutron powder diffraction pattern of  $\zeta$ -glycine at 100 K (blue = observed, red = calculated). In addition to the peaks  $\zeta$ -glycine, the pattern also shows the presence of residual  $\varepsilon$ - and a trace of  $\gamma$ -glycine. Other peaks arise from the sample environment, namely the pressure marker and the  $\text{Al}_2\text{O}_3$  and  $\text{ZrO}_2$  components of the anvils of the pressure cell. (b) Rietveld fit of the neutron powder diffraction pattern of  $\beta$ -glycine (contaminated with  $\zeta$ - and a trace of  $\gamma$ -glycine) at 290 K. A 1 Å  $d$  spacing approximates to 4837  $\mu\text{s}$  in time-of-flight.

E Kucukbenli, CH Pham, SdG,  
C Bull, G Flowitt-Hill, HY Playford, M Tucker, S Parsons  
Int Union Crist J 4, 569–574 (2017)

Exploring the phase space for larger molecules (ex. CLR) requires fast and accurate energetics

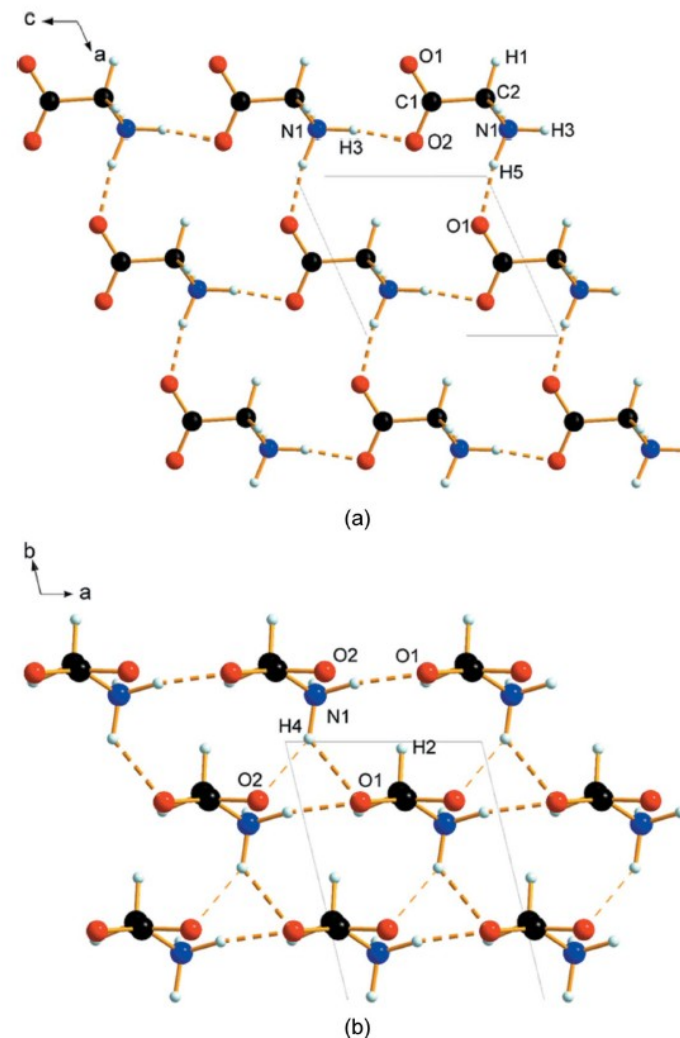


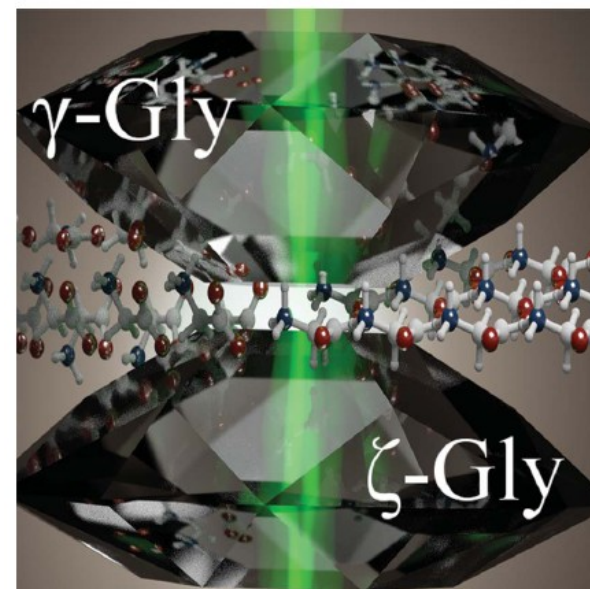
Figure 3

Intermolecular interactions in  $\zeta$ -glycine. (a) Layers formed in the  $ac$  plane, viewed along  $b$ . (b) Stacking of the layers, viewed along  $c$ .

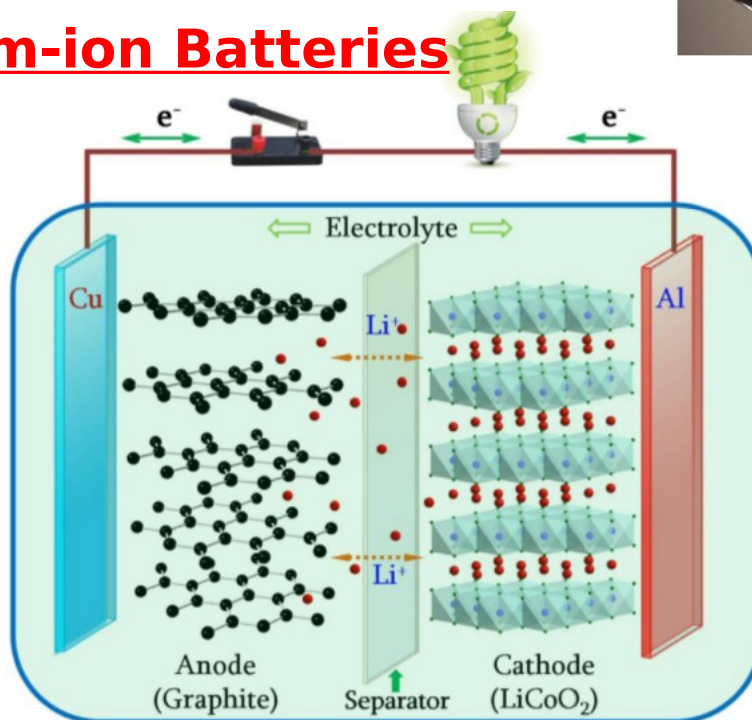
## Complete $^{13}\text{C}$ Chemical Shift Assignment for Cholesterol Crystal



## $\zeta$ -Glycine: Insight into the mechanism of a polymorphic phase transition

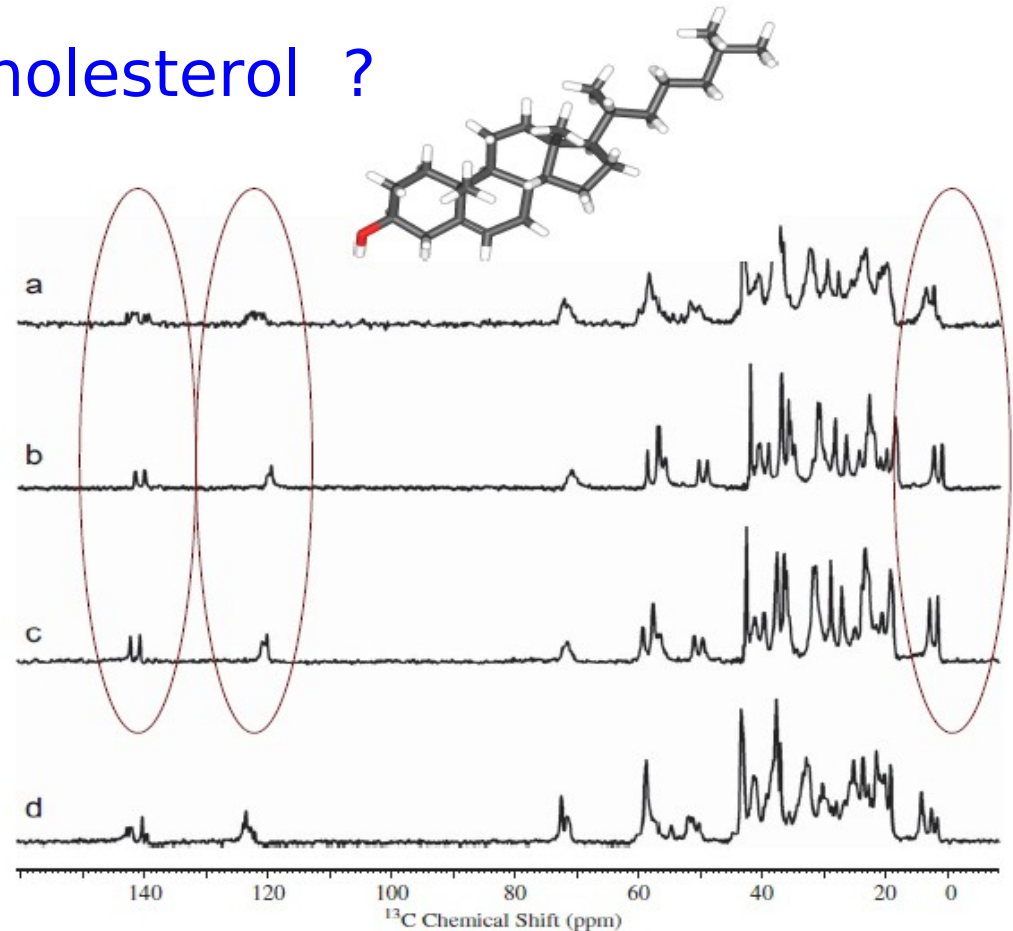
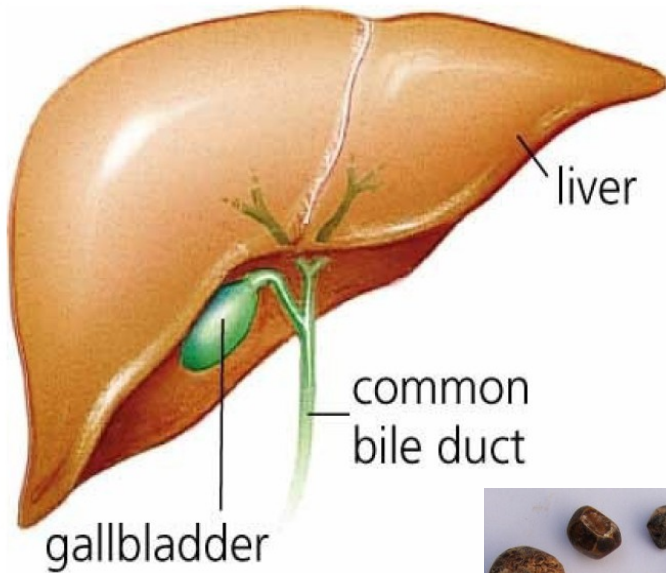


## Lithium-ion Batteries

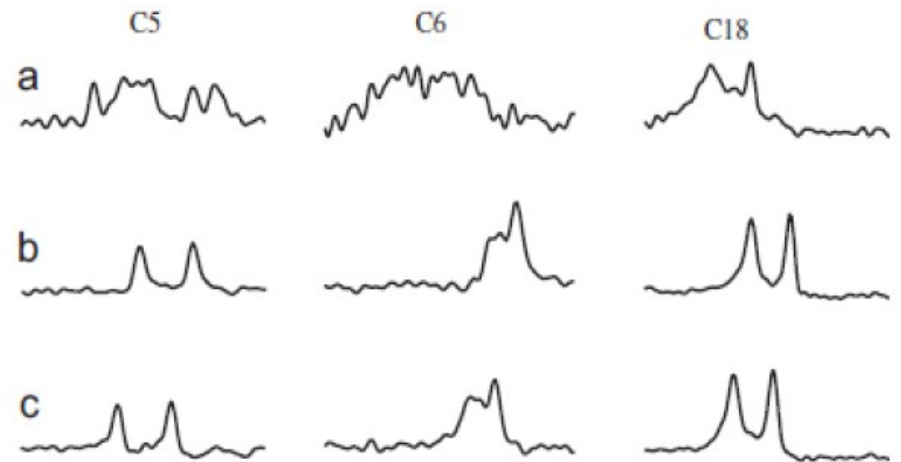


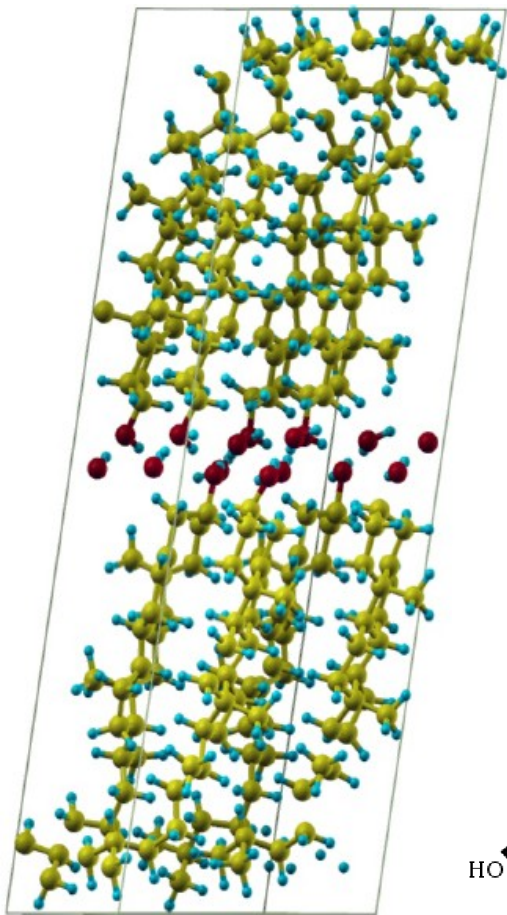


# Why Cholesterol ?

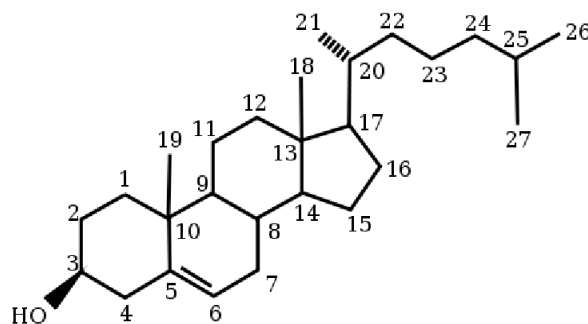


- a) Gallbladder Cancer
- b) Chronic Cholecystitis
- c) Xantho-Granulomatous Cholecystitis

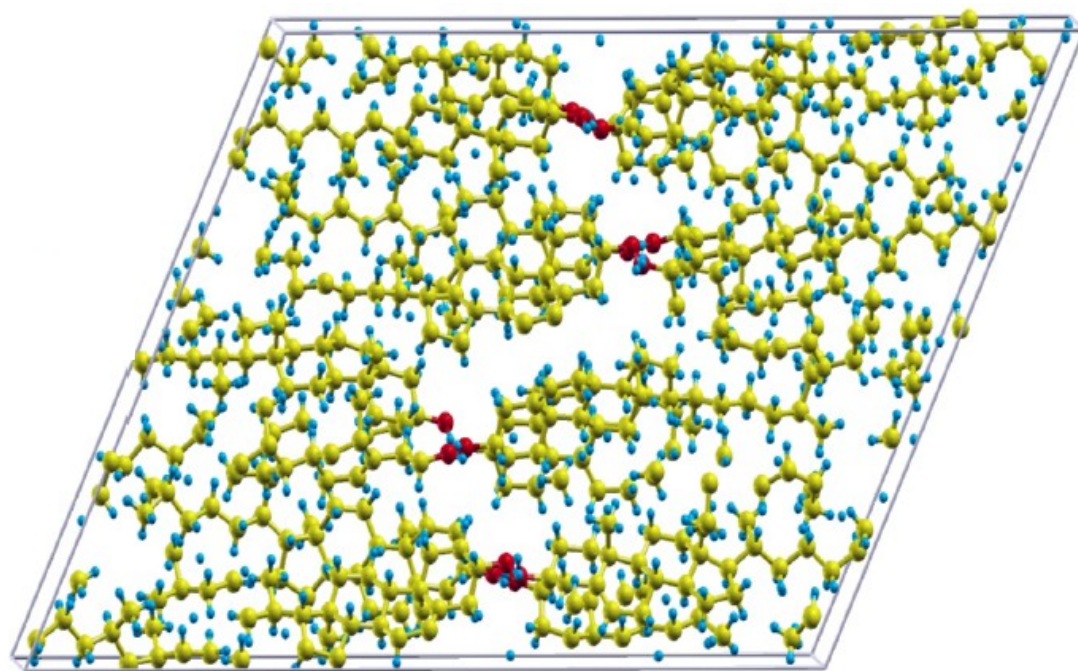




**Monohydrate Cholesterol (ChM)**  
 8 CLR + 8 w molecules - 616 atoms



**High temperature Anhydrous Cholesterol (ChAh)**  
 16 CLR mol - 1184 atoms



**Low temperature Anhydrous Cholesterol (ChAl)**  
 8 CLR mol - 592 atoms

(not shown)

# Lithium Interaction with Graphene-like Materials



~10Wh



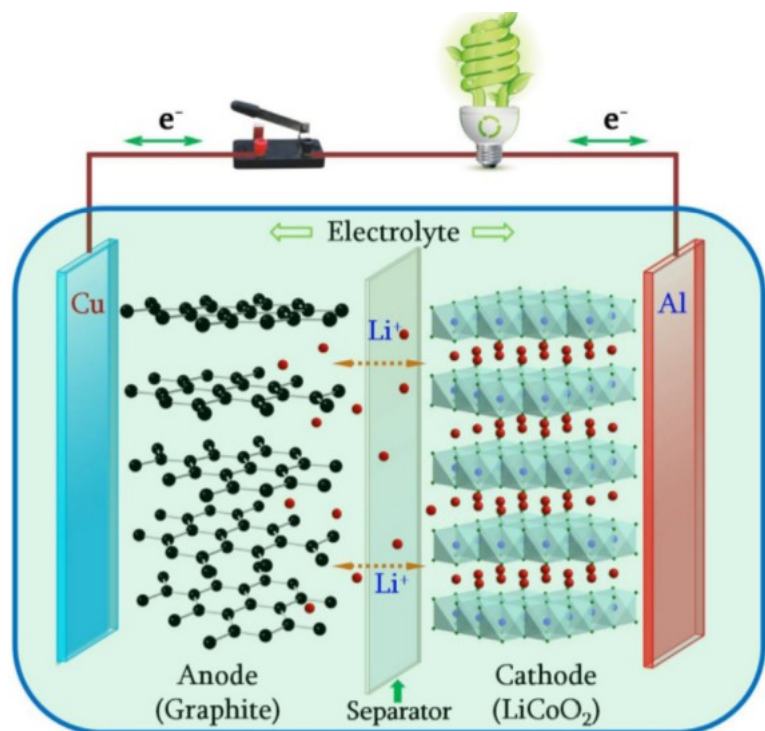
~100Wh



~10,000Wh



# Lithium ion batteries



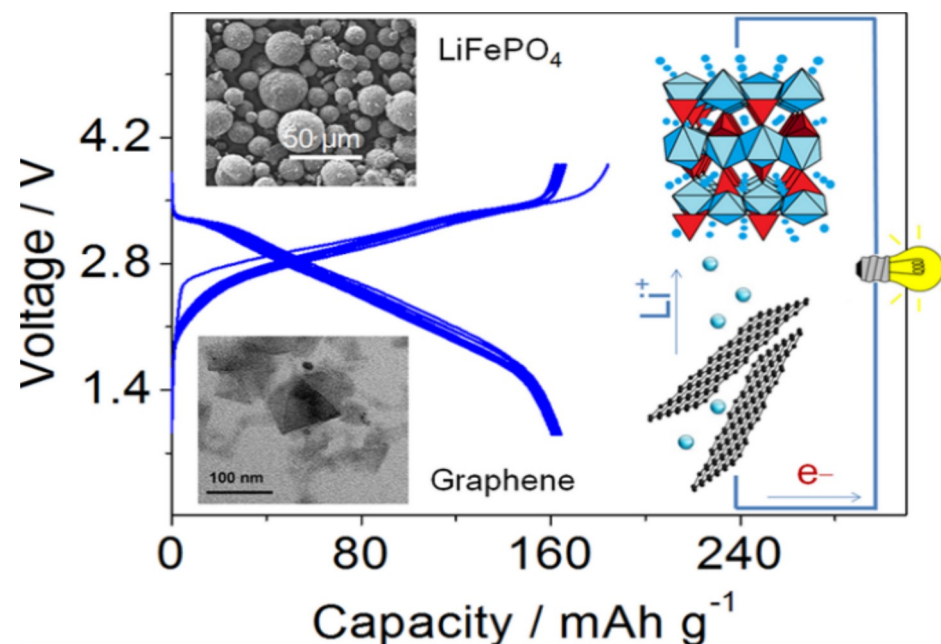
- Cathode: Source of lithium
- Electrolyte: Ionic conductivity
- Anode: Lithium holder
- Current collectors

**Capacity:** The amount of Li absorbed by anode

- Stoichiometry of Li adsorbed graphite is  $\text{LiC}_6$

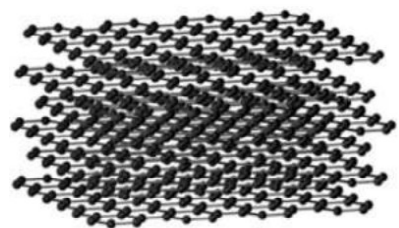
**Alternative anode materials :**

Graphene due to its large surface to mass ratio and good electrical conductivity.

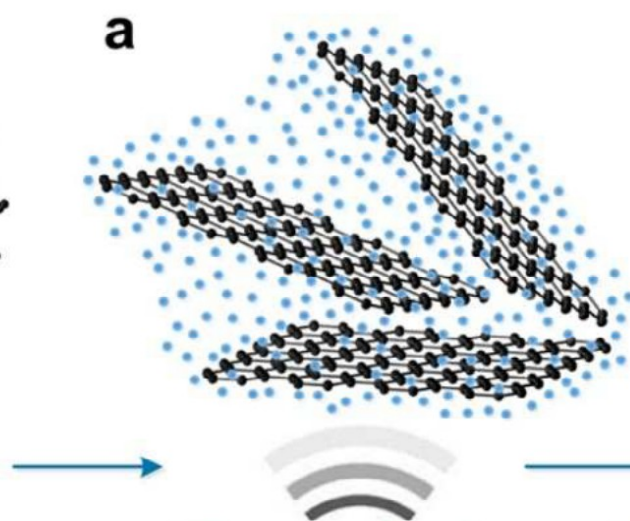


- graphene nanoflakes as alternative anode
- Flakes ~30-100 nm lateral dimension
- **Very high Li uptake:  $\text{LiC}_2$**

Hassoun et al. Nano Lett. 2014, 14, 4901-4906



Graphite



Ultrasonication



Ultracentrifugation



Graphene  
ink

Traditionally model potentials construction requires a lot of physical intuition and are strongly dependent on the available experimental information.

Not transferable to experimentally unexplored regions.


Limited accuracy due to rigid functional form.

DFT is a viable option to gather accurate information but requires a systematic approach to build a potential that can incorporate its features.



**Artificial  
Intelligence**  
is better than none

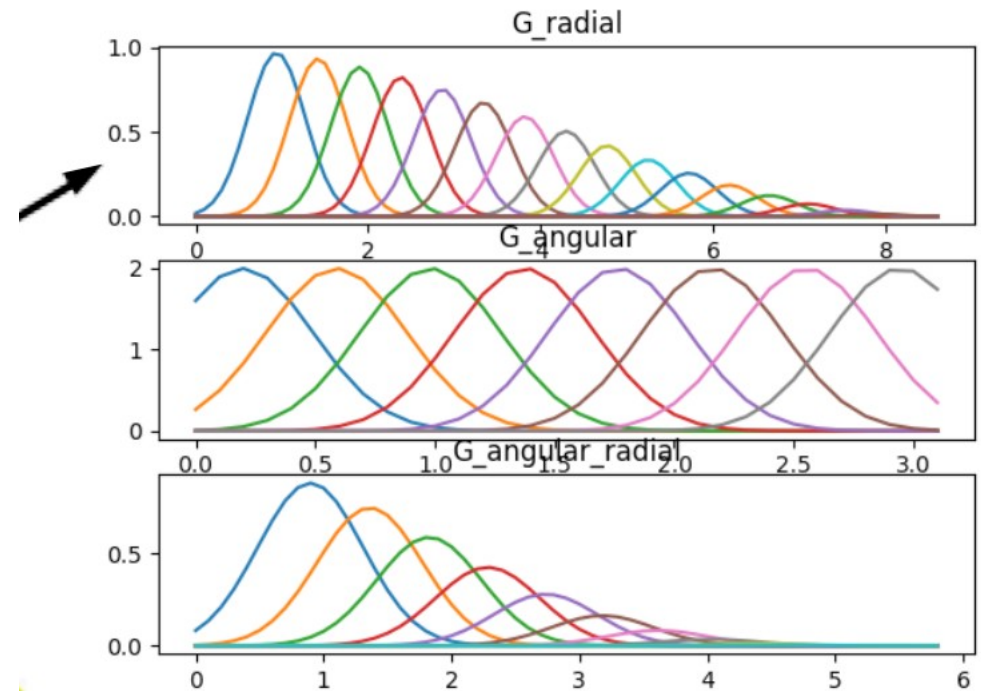
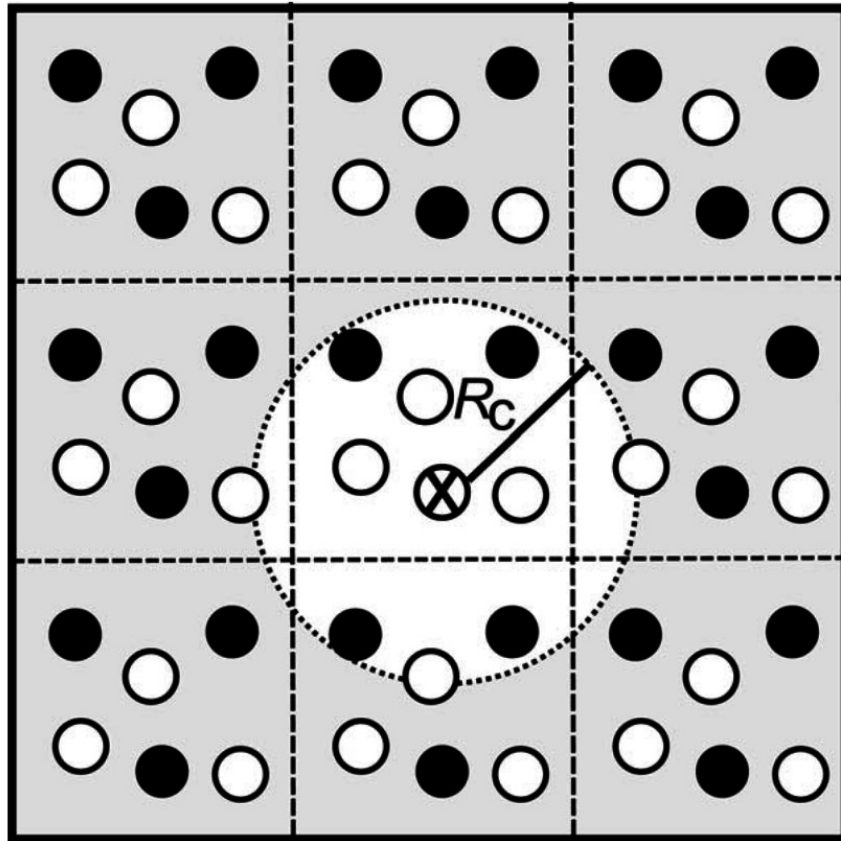
Replace the expensive DFT total energy calculations (or other accurate methods) with an interatomic potentials built to reproduce DFT data in a variety of environments

$$E(c) = \sum_{\alpha} \sum_{i \in \alpha} \varepsilon_{\alpha}(\mathbf{d}_i) + \text{long range contrib}$$


- Kernel Ridge Regression (and Gaussian Processes)
- Neural Networks
- local environment descriptors



## - Modified Behler-Parrinello descriptor



# Symmetry Functions

The radial part

$$G^R = \sum_{j \neq i} e^{-\eta(R_{ij}-R_s)^2} f_c(R_{ij})$$

The angular part

$$G^A = 2^{1-\xi} \sum_{jk \neq i} (1 + \cos(\theta_{ijk} - \theta_s))^\xi e^{-\eta(\frac{R_{ij}+R_{ik}}{2}-R_s)^2} f_c(R_{ij}) f_c(R_{ik})$$

$$f_c(R) = \frac{1}{2} \left( 1 + \cos\left(\frac{\pi R}{R_c}\right) \right)$$

J. Behler and M. Parrinello, Phys. Rev. Lett. **98**, 146401 (2007)

J.S.Smith, O.Isayev and A.E.Roitberg, Chem. Sci., 2017, **8**, 3192-3203

# Representation

$$G_{m,s;i}^R = \sum_{i \neq j}^{\text{All atoms kind s}} e^{-\eta(r_{ij}-R_m)^2} f_c(r_{ij})$$

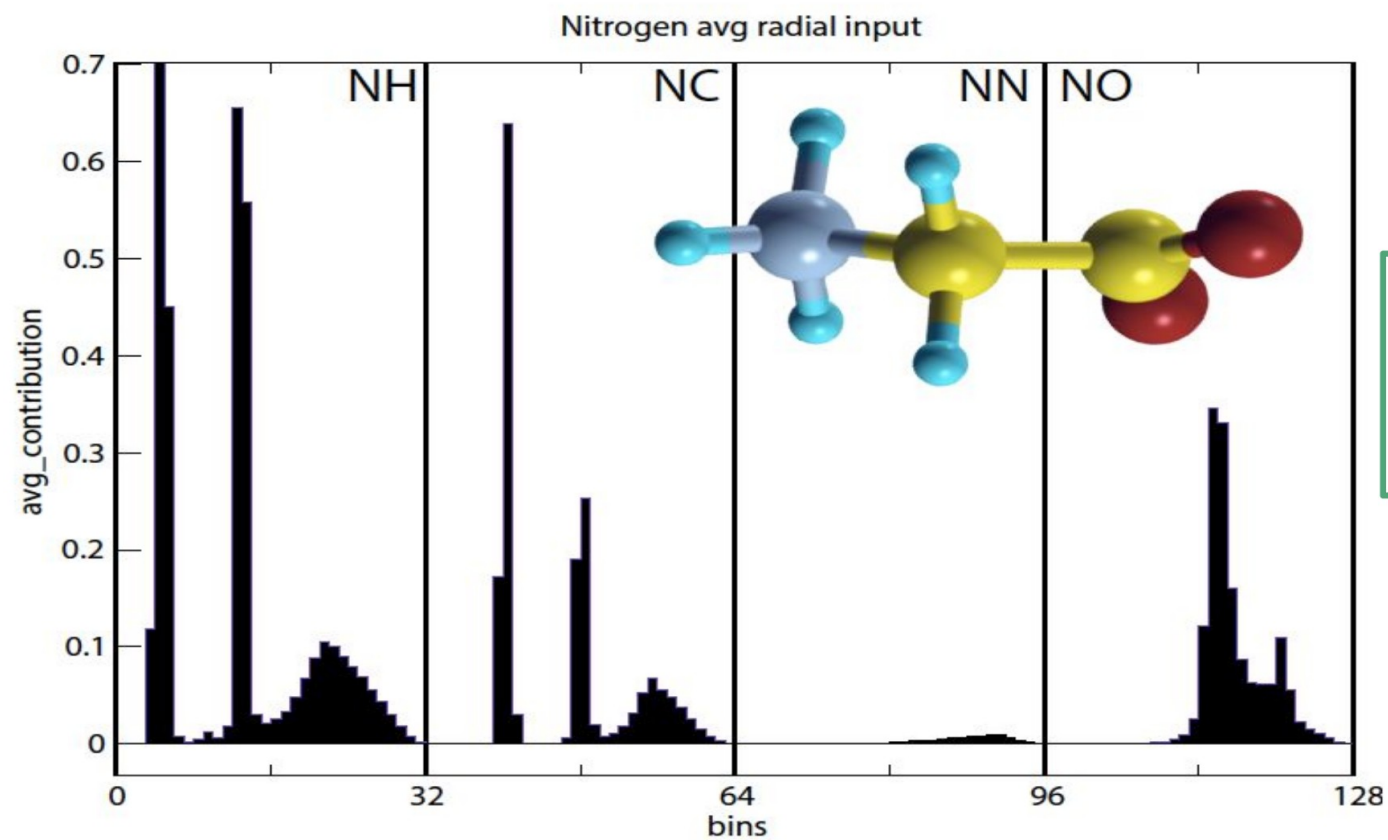
$$f_c(r_{ij}) = \begin{cases} 0.5 \left[ \cos \left( \frac{\pi r_{ij}}{R_c} \right) + 1 \right] & \text{if } r_{ij} \leq R_c \\ 0 & \text{if } r_{ij} \geq R_c \end{cases}$$

$R_0=0.5\text{\AA}$  ,  $R_c= 4.6\text{\AA}$   
32 bins per pair:  
32x4=128 parameters

J. Behler and M. Parrinello, PRL, 98.14 (2007).

Smith et al, Chem Sci 8 3192 (2017)  
DOI: 10.1039/c6sc05720a

# Average G-radial for N in GLY



$R_0=0.5\text{\AA}$  ,  $R_c= 4.6\text{\AA}$   
32 bins per pair:  
 $32 \times 4 = 128$  parameters

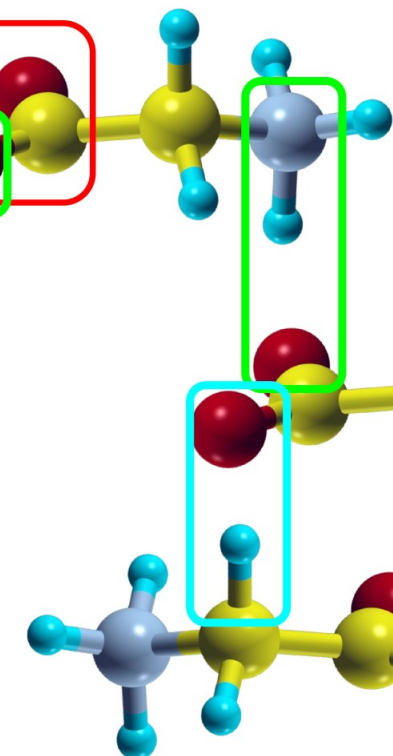
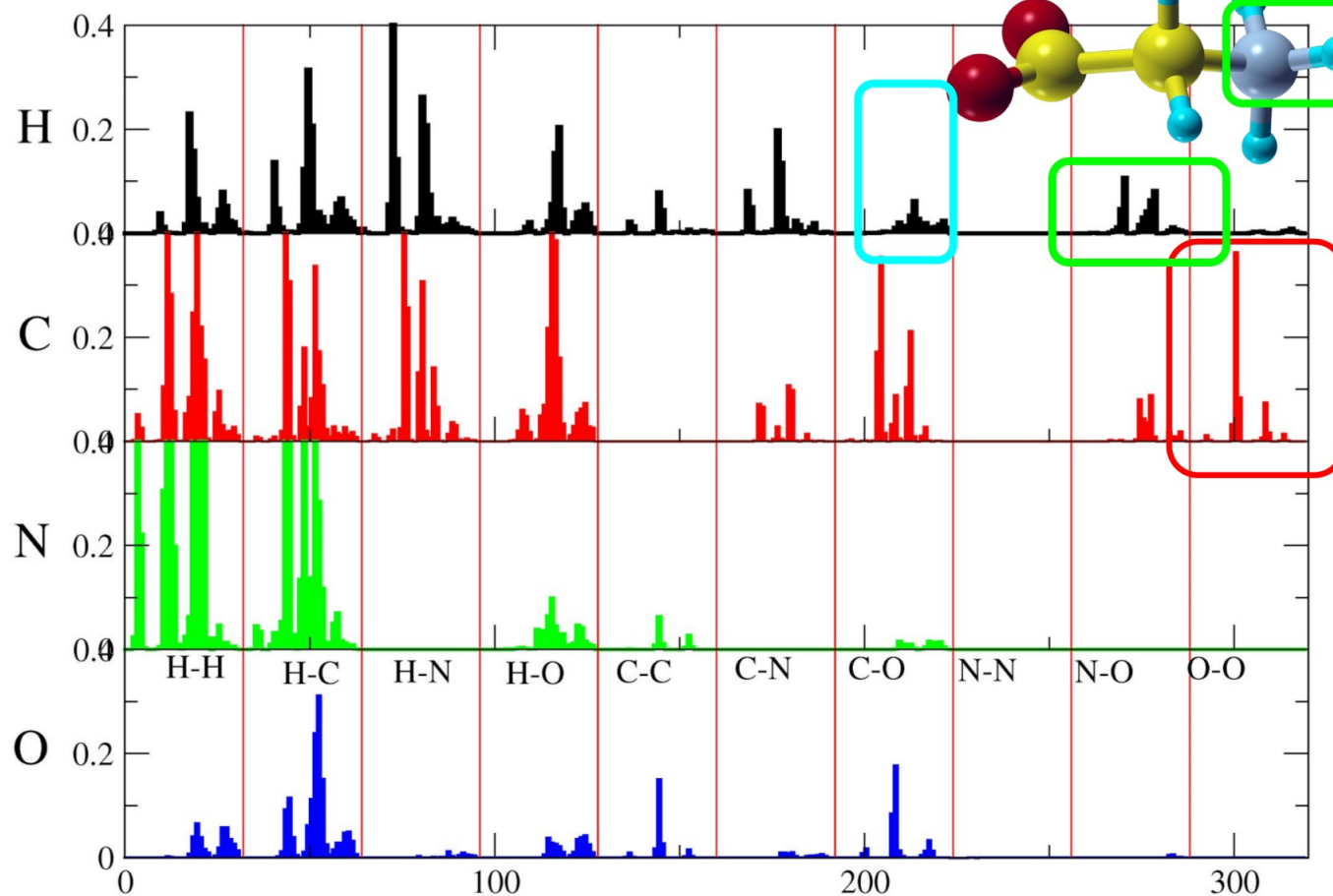
# Representation

$$G_{n,m,s;i}^A = 2^{1-\xi} \sum_{\substack{\text{All atom of kind s} \\ j,k \neq i}} (1 + \lambda \cos(\Theta_{ijk} - \Theta_n))^\xi e^{-\eta \left( \frac{r_{ij} + r_{ik}}{2} - R_m \right)^2} f_c(r_{ij}) f_c(r_{ik})$$

Smith et al, Chem Sci (2016)  
DOI: 10.1039/c6sc05720a

$R_0=0.5\text{\AA}$  ,  $R_c= 3.1\text{\AA}$   
8 angular bin for each 8 radial bin  
64 bins per trimer:  
 $64 \times 10 = 640$  parameters

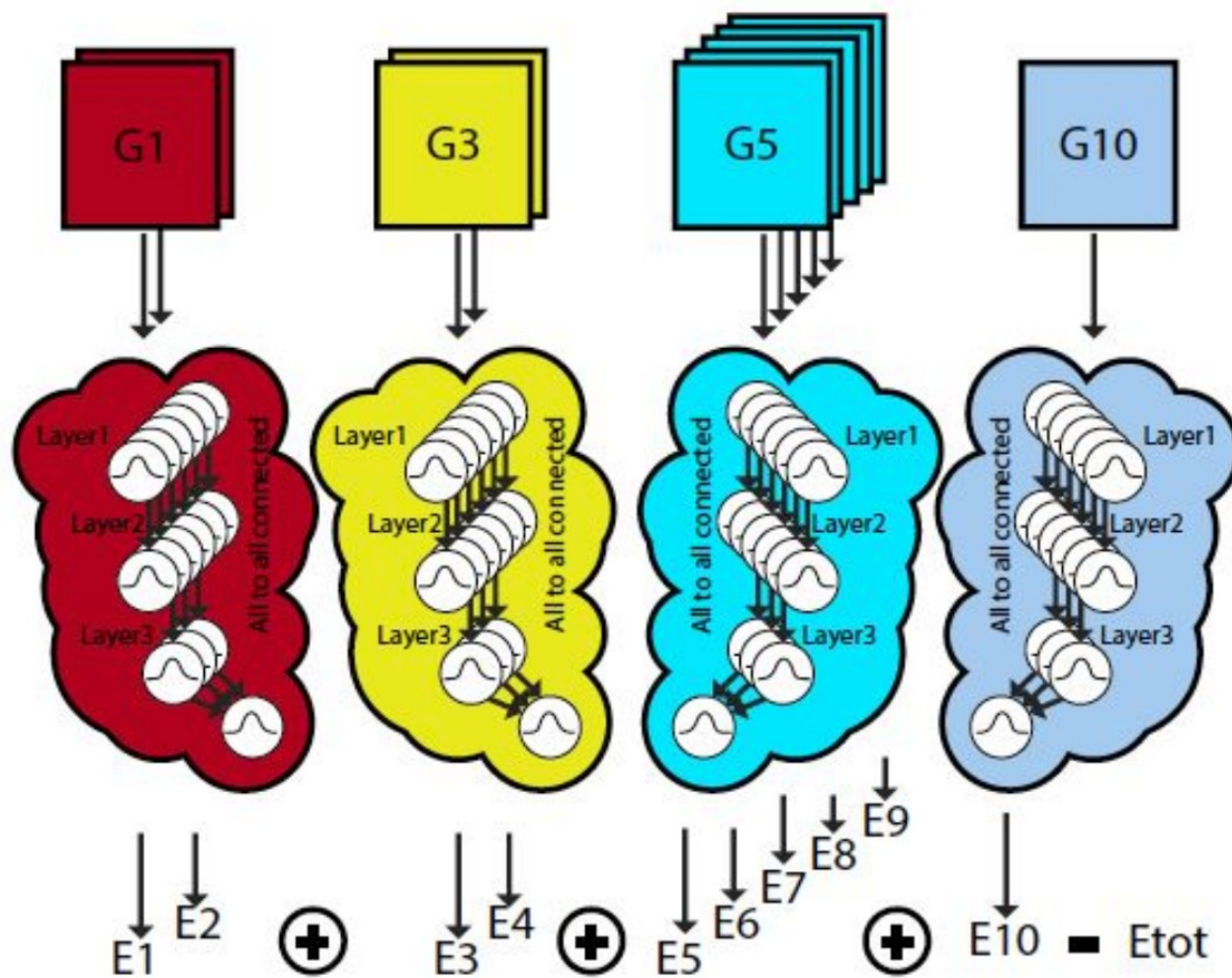
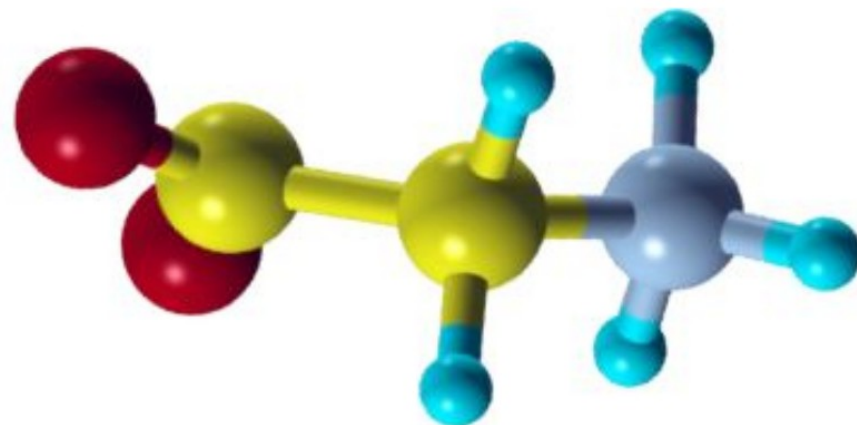
# Average G-angular in GLY



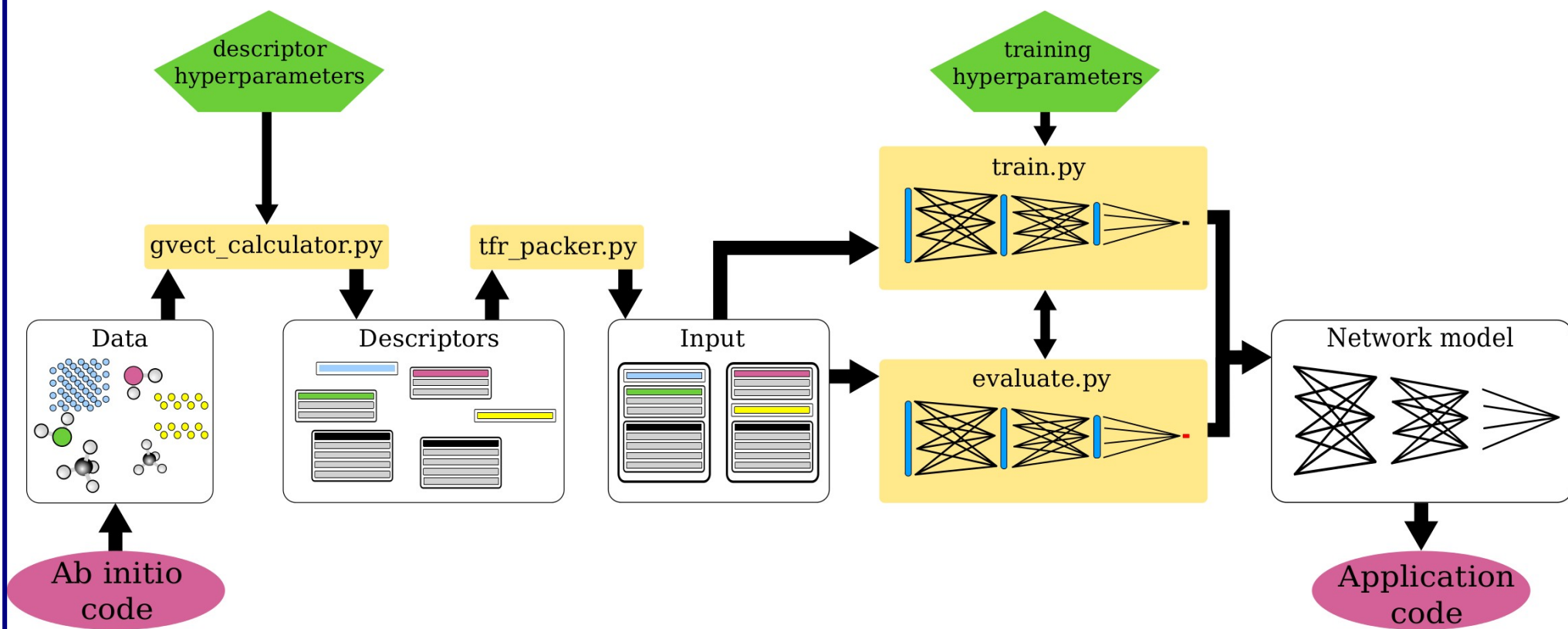
Halved version:  
 8 angular for 4 radial  
 32 per trimer  
 $32 \times 10 = 320$  parameters



# GLY



# PANNA workflow



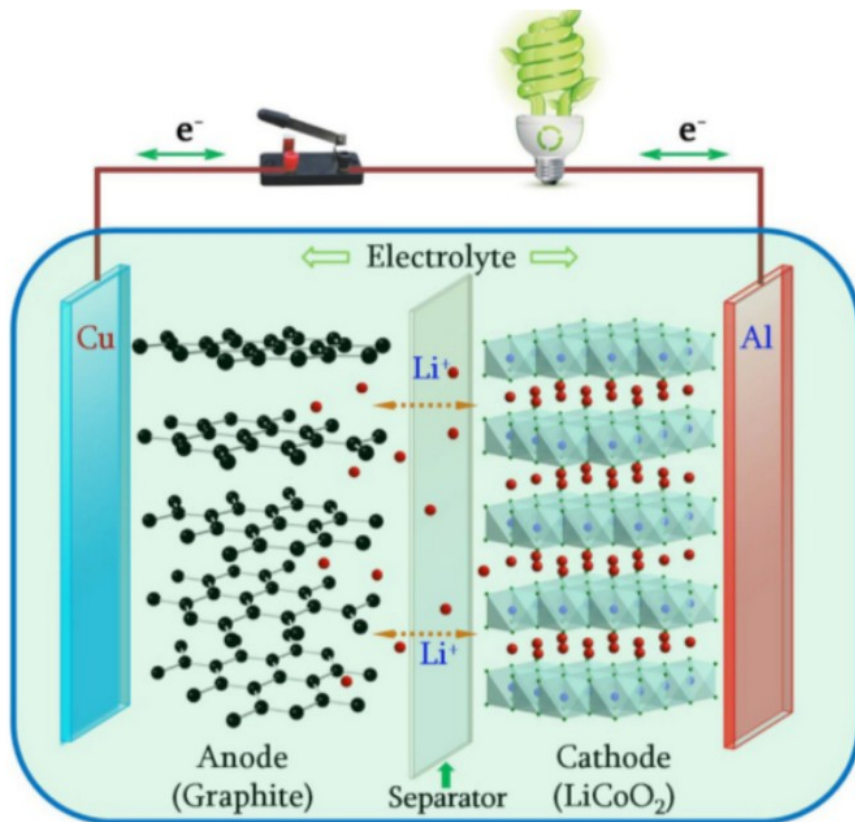
R Lot, F Pellegrini, Y Shaidu, E Kucukbenli, *arXiv:1907.03055*

<https://gitlab.com/pannadevs/panna>



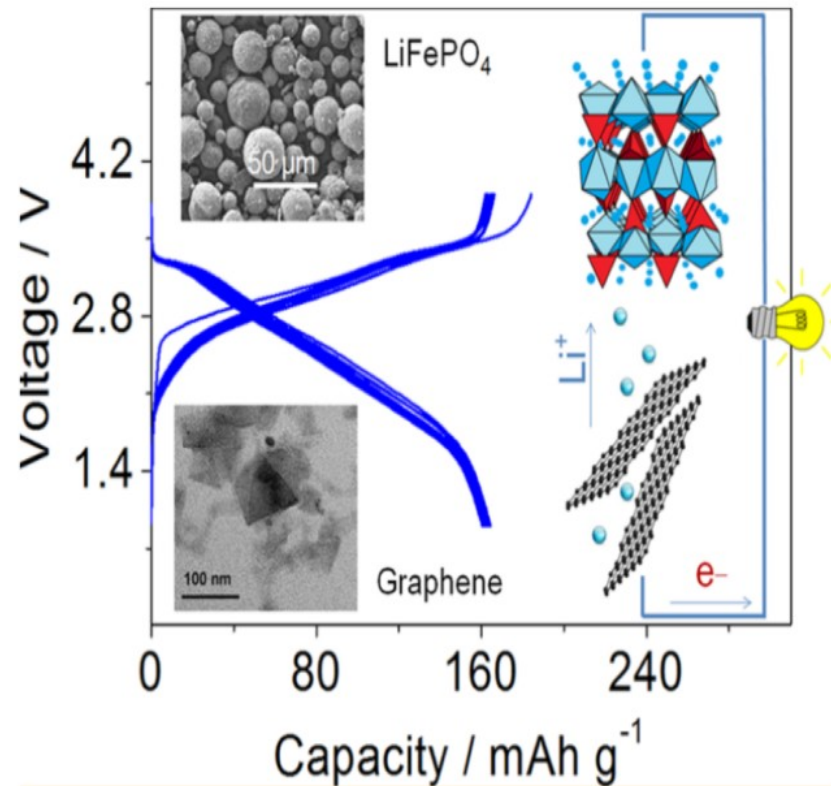


# Lithium ion batteries



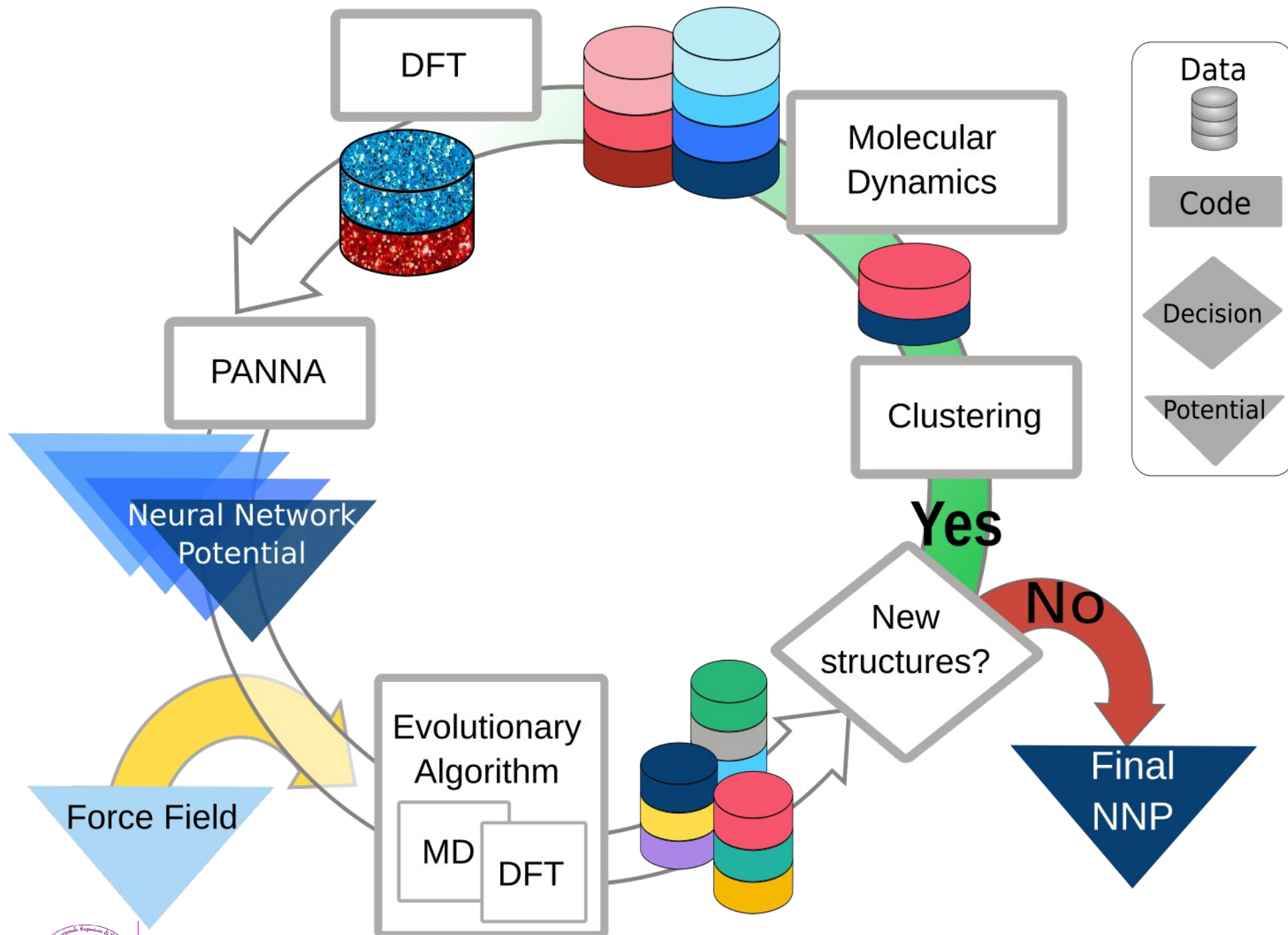
- graphite:  $\text{LiC}_6$

Today 19(2):109-123, 2016

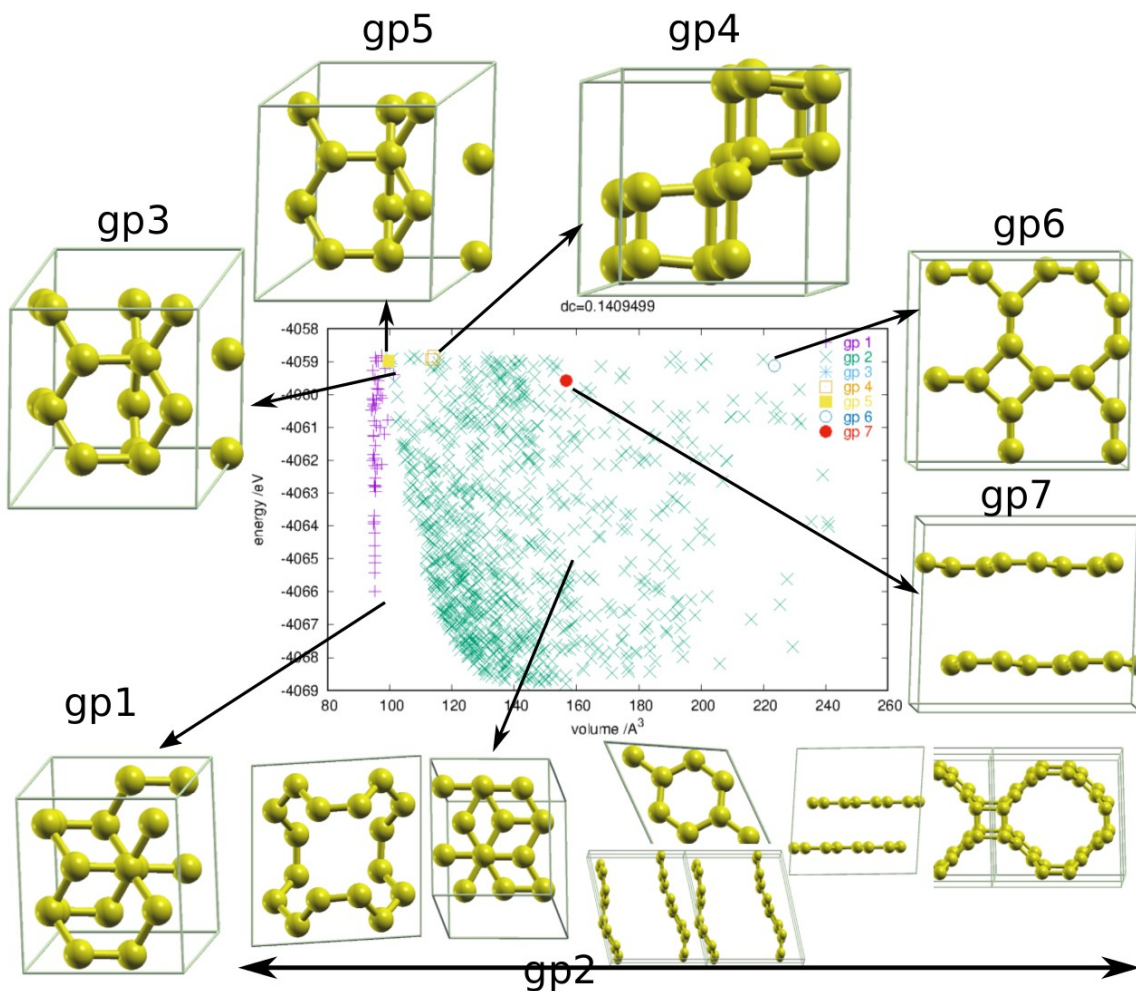


- graphene:  $\text{LiC}_2$

Hassoun et al. Nano Lett. 2014, 14, 4901-4906



# Carbon Systems



$$D = \frac{1}{2} \left( 1 - \frac{\mathbf{F}_1 * \mathbf{F}_2}{|\mathbf{F}_1| |\mathbf{F}_2|} \right)$$

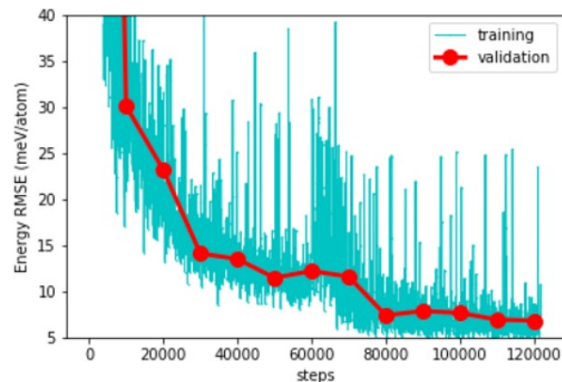
## Training Parameters

- Architectures: 144:64:32:1
- Activation function: gaussian:gaussian:linear
- minimized quantity:

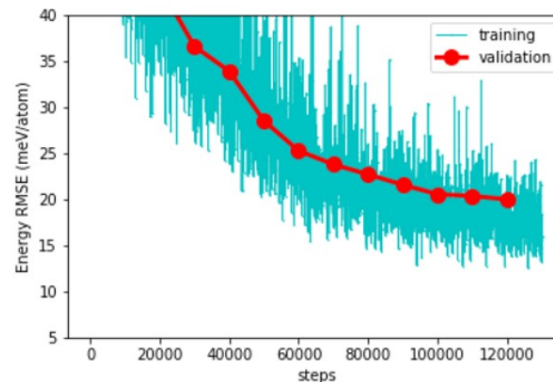
$$Loss = E_{Loss} + \beta F_{Loss}$$

# Carbon Systems: training and validation

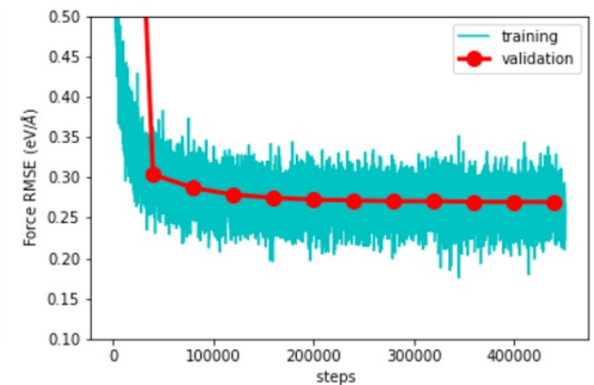
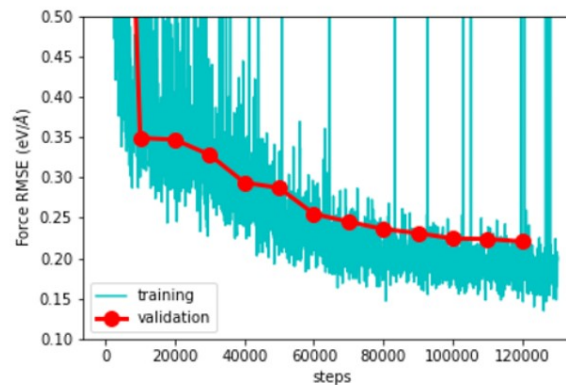
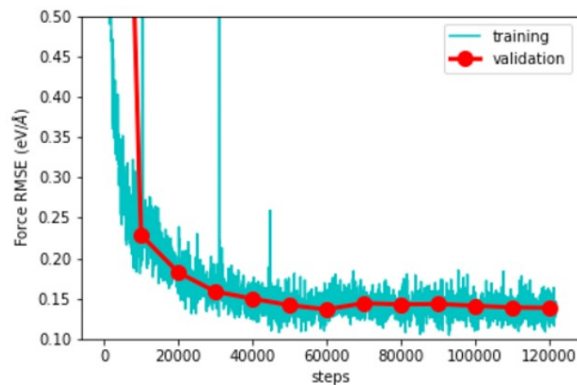
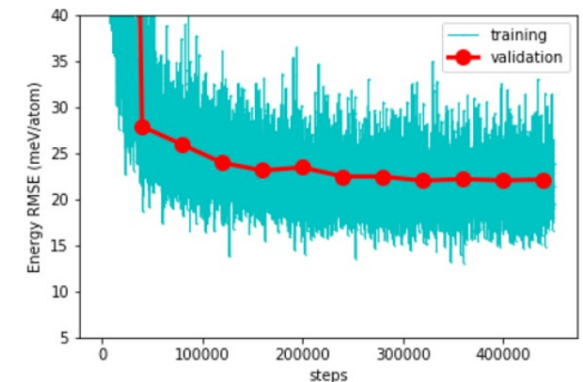
## 1st iteration



## 2nd iteration



## 3rd iteration

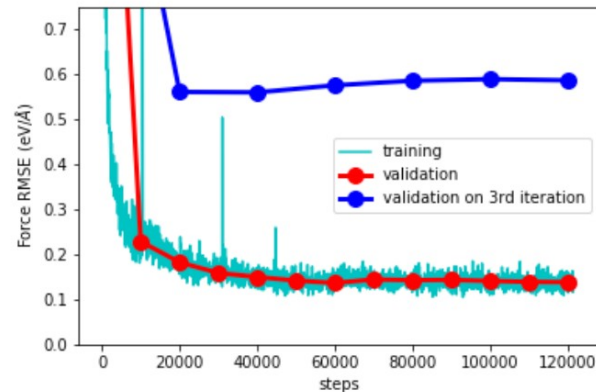
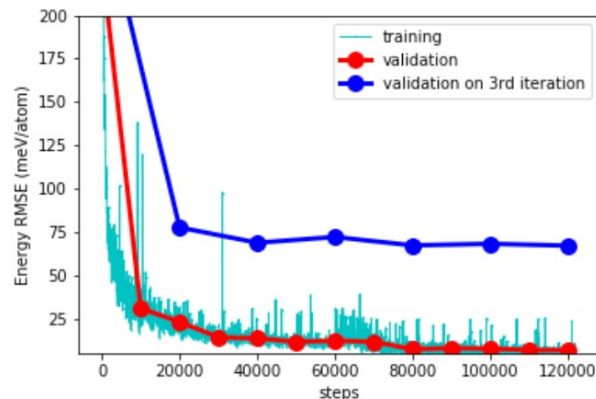


- 20 % of the data set is set aside for validation

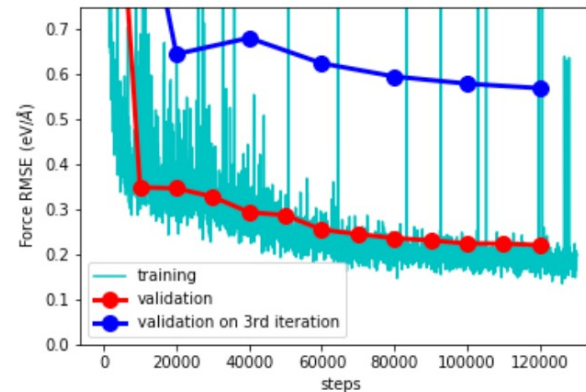
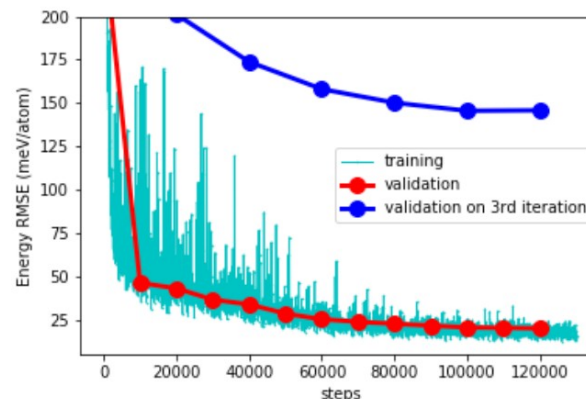


# Carbon Systems: training and validation

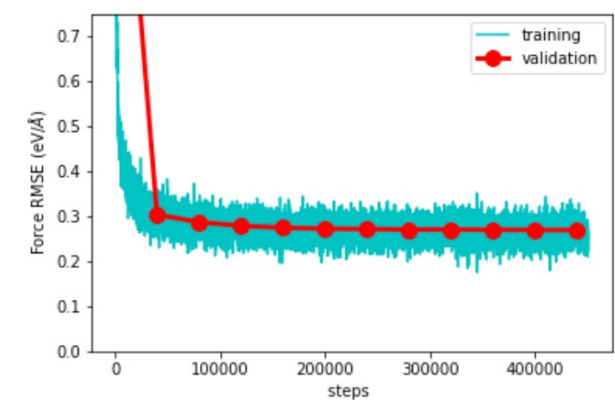
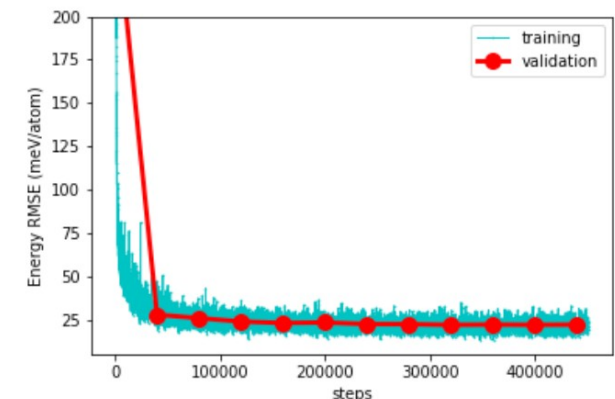
## 1st iteration



## 2nd iteration



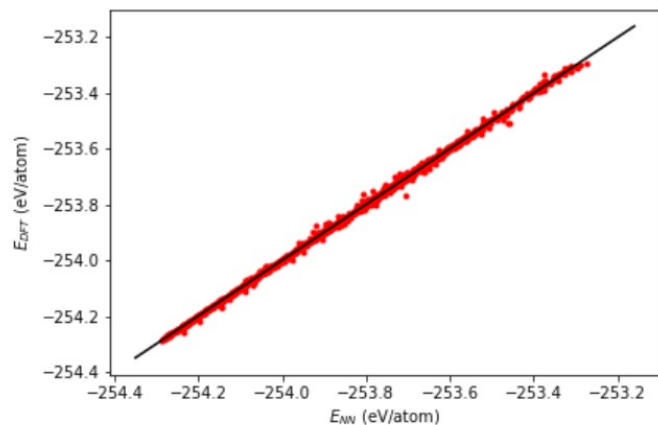
## 3rd iteration



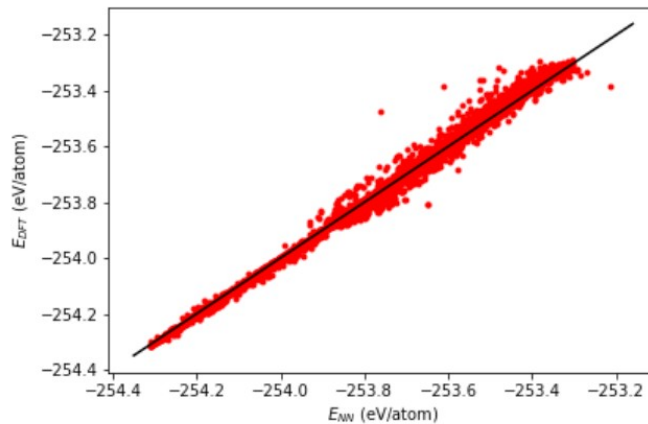
- 20 % of the data set is set aside for validation

## Error distribution: energies

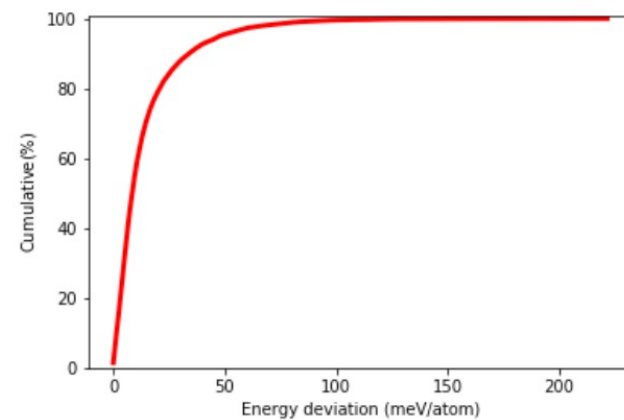
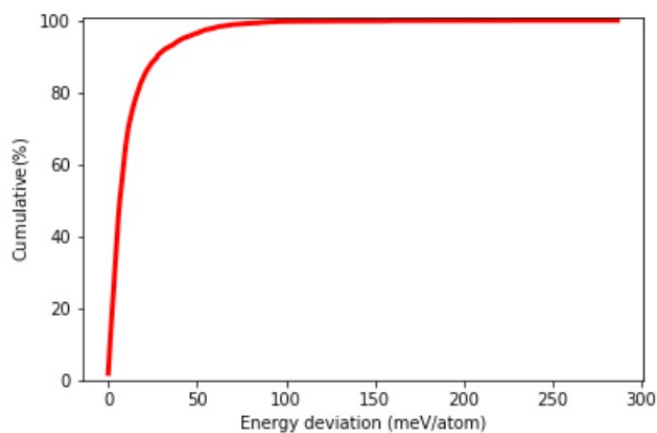
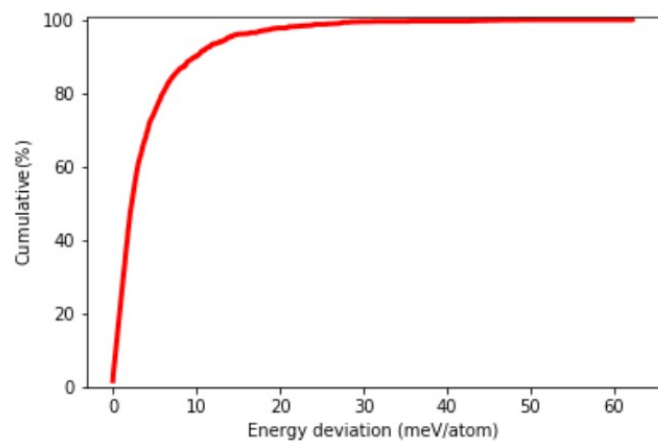
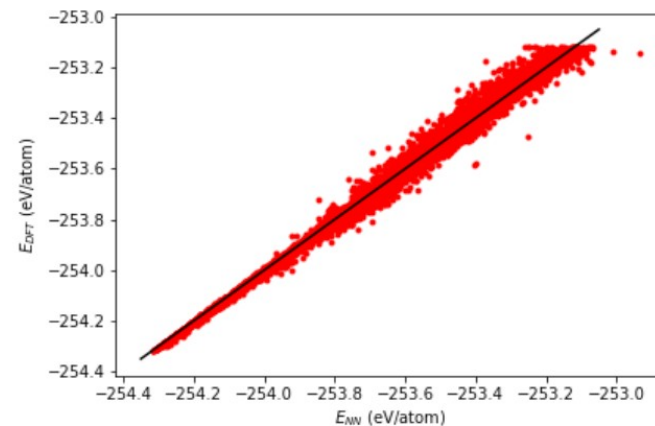
### 1st iteration



### 2nd iteration

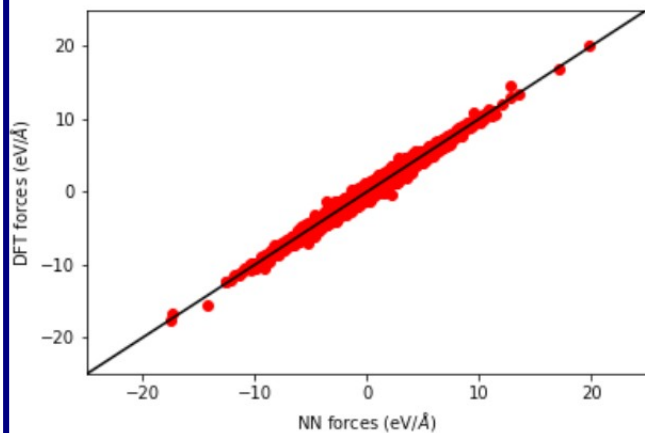


### 3rd iteration

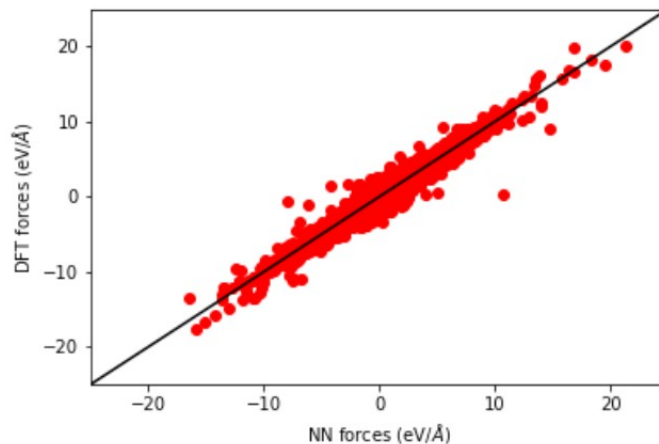


## Error distribution: forces

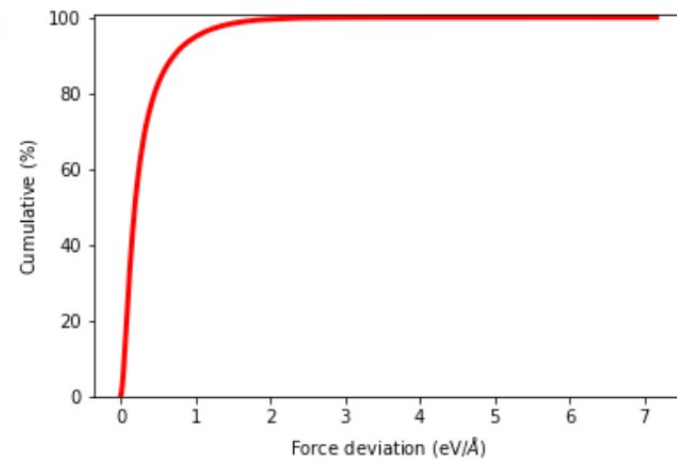
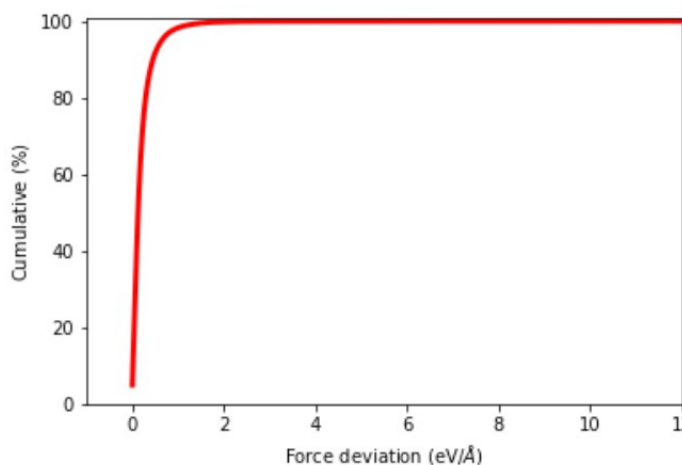
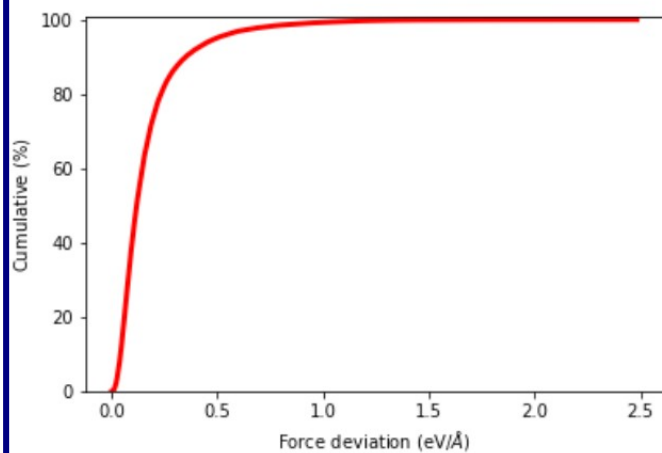
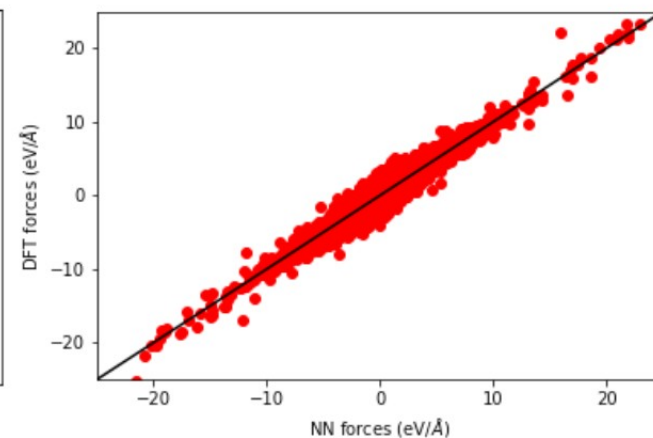
### 1st iteration



### 2nd iteration



### 3rd iteration



## Effect of diversity on training and validation RMSE

| Train \ Validate | T error | All D   | $D < 0.15$ | $D < 0.10$ | $D < 0.05$ | $D_{12} < 0.05$ |
|------------------|---------|---------|------------|------------|------------|-----------------|
| All D            | 22.070  | 22.131  | 20.938     | 15.161     | 7.659      | 7.302           |
| $D < 0.15$       | 18.066  | 80.424  | 18.422     | 13.342     | 5.949      | 17.567          |
| $D < 0.10$       | 8.563   | 162.327 | 52.178     | 9.369      | 4.391      | 76.260          |
| $D < 0.05$       | 2.633   | 879.207 | 452.598    | 89.022     | 2.585      | 650.075         |
| $D_{12} < 0.05$  | 2.574   | 174.257 | 88.311     | 51.972     | 2.739      | 2.627           |

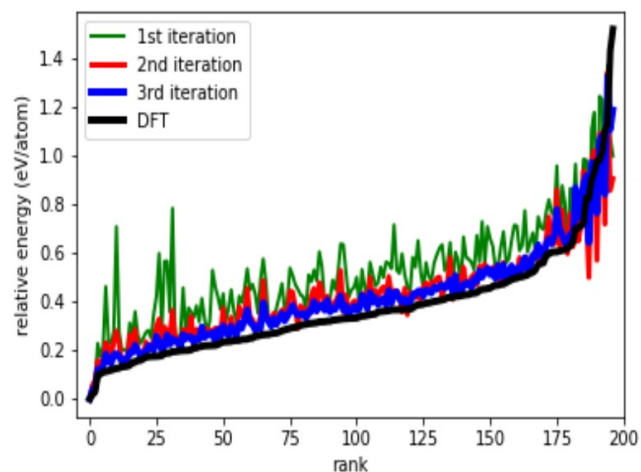
| Train \ Validate | All D  | $D < 0.15$ | $D < 0.10$ | $D < 0.05$ | $D_{12} < 0.05$ |
|------------------|--------|------------|------------|------------|-----------------|
| All D            | 0.2696 | 0.2717     | 0.1974     | 0.0829     | 0.0785          |
| $D < 0.15$       | 0.5969 | 0.2523     | 0.1789     | 0.0766     | 0.1873          |
| $D < 0.15$       | 0.9571 | 0.4410     | 0.1472     | 0.0617     | 0.3112          |
| $D < 0.15$       | 3.2641 | 2.0028     | 0.7243     | 0.0529     | 0.8699          |
| $D_{12} < 0.05$  | 0.9641 | 0.8934     | 0.5440     | 0.0529     | 0.0504          |



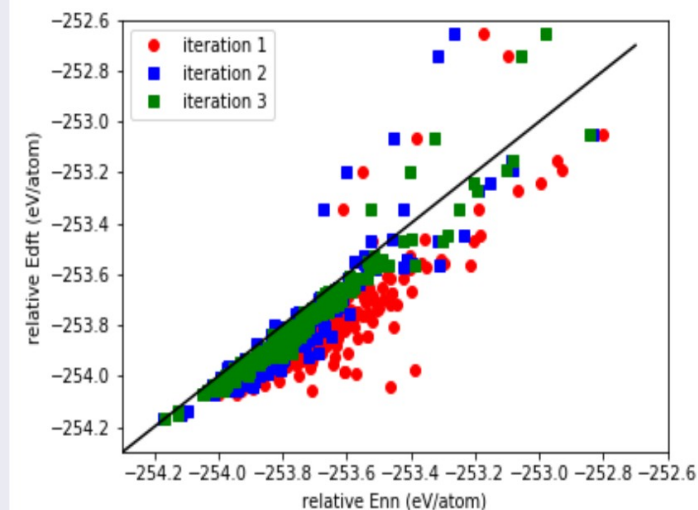
## Energy ordering of test structures

- 197 different  $sp^3$  C structures<sup>3</sup>

### Ordering



### energy correlation

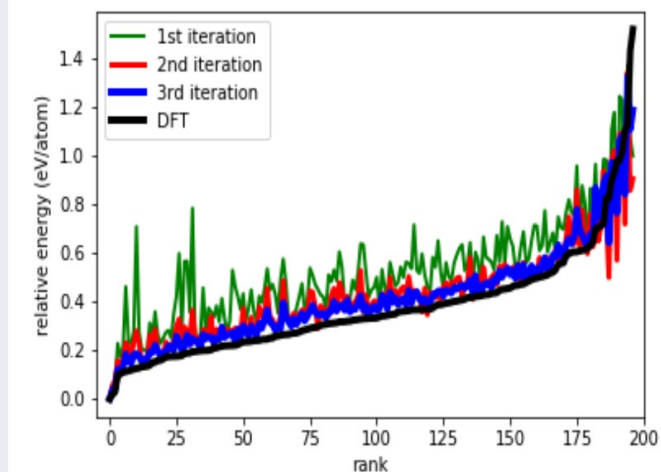


<sup>3</sup>V.L. Deringer, G. Csanyi and D.M. Proserpio, Chem. Phys. Chem. 2017, **18**, 873–877

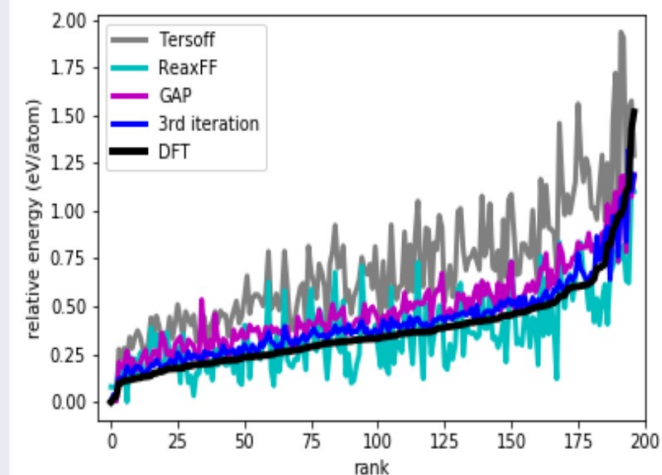
## Energy ordering of test structures

- 197 different  $sp^3$  C structures<sup>4</sup>

### Ordering



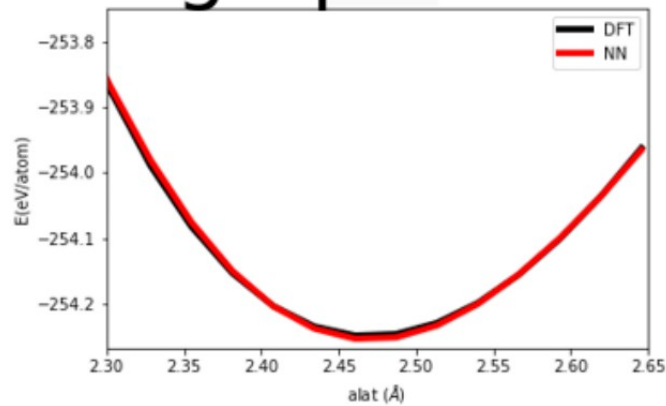
### NN vs force fields



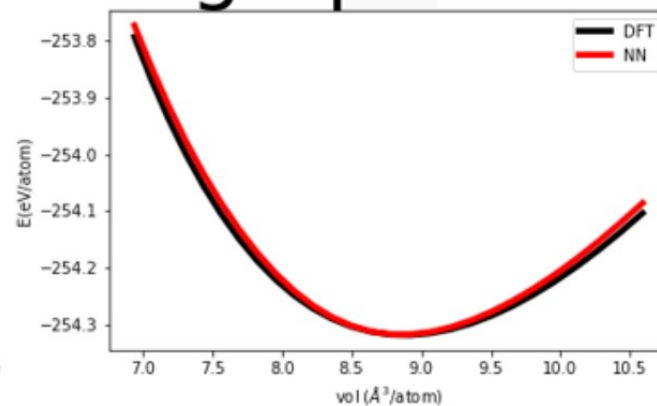
<sup>4</sup>V.L. Deringer, G. Csanyi and D.M. Proserpio, Chem. Phys. Chem. 2017, **18**, 873–877

## Equation of State

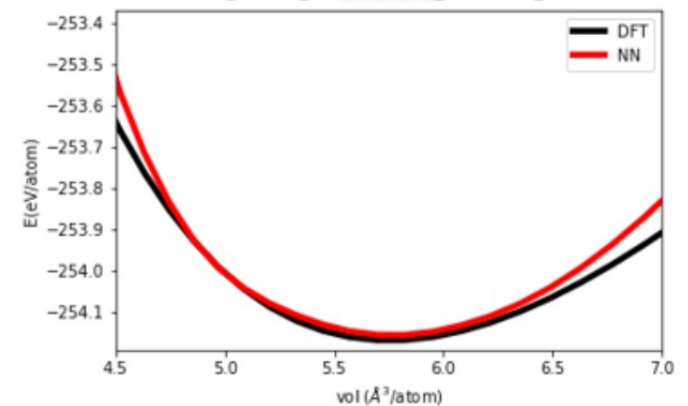
graphene



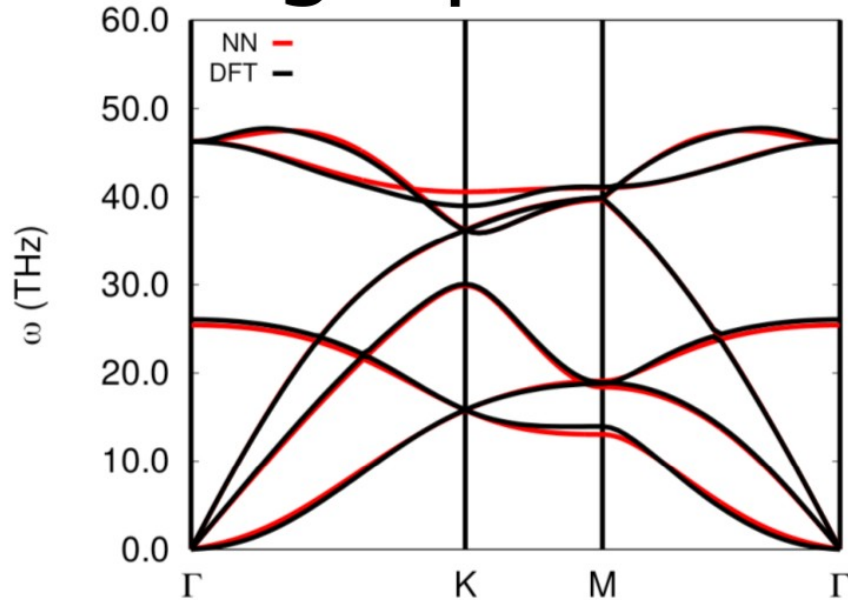
graphite



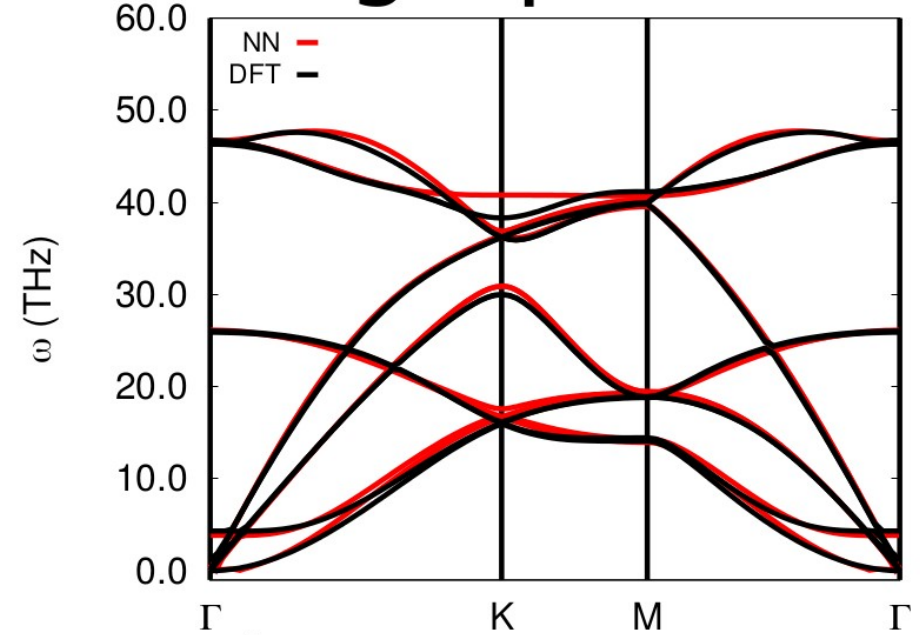
diamond



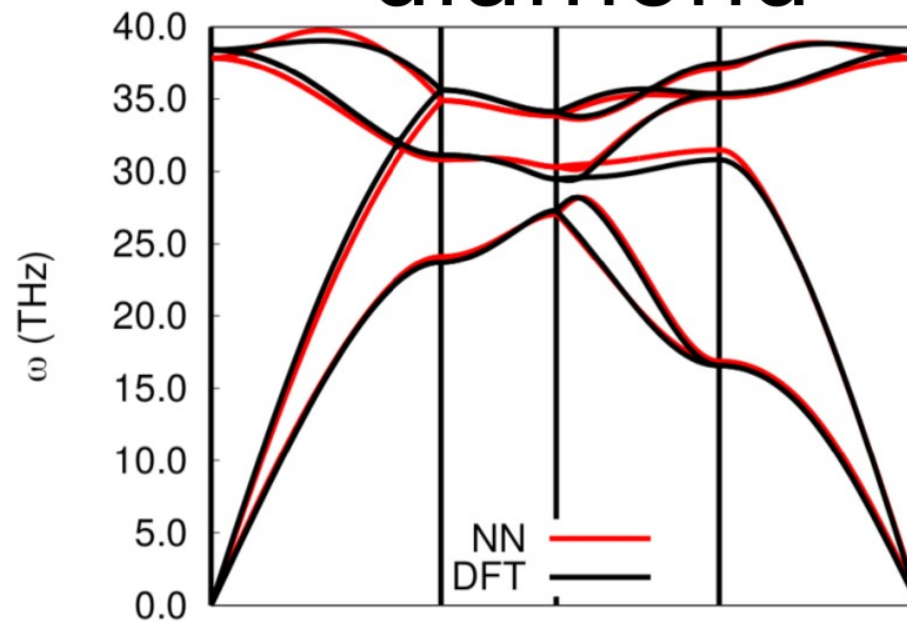
# graphene



# graphite

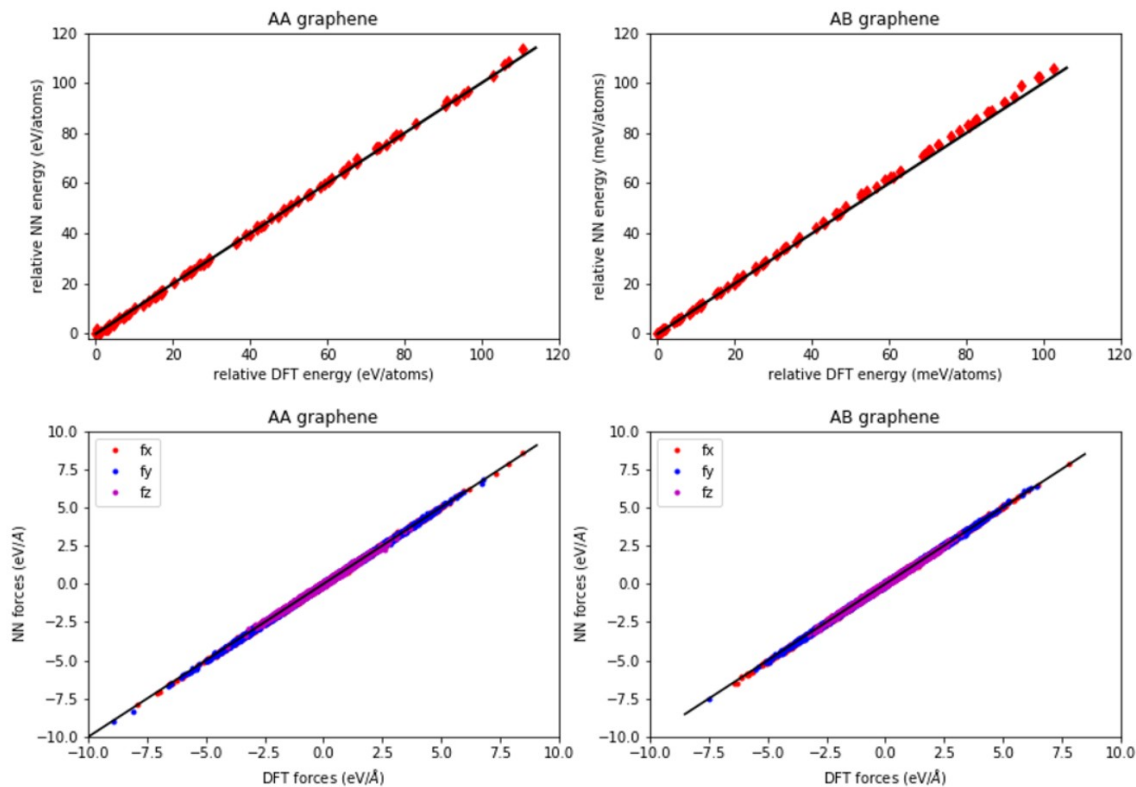


# diamond



# Bilayer Graphene

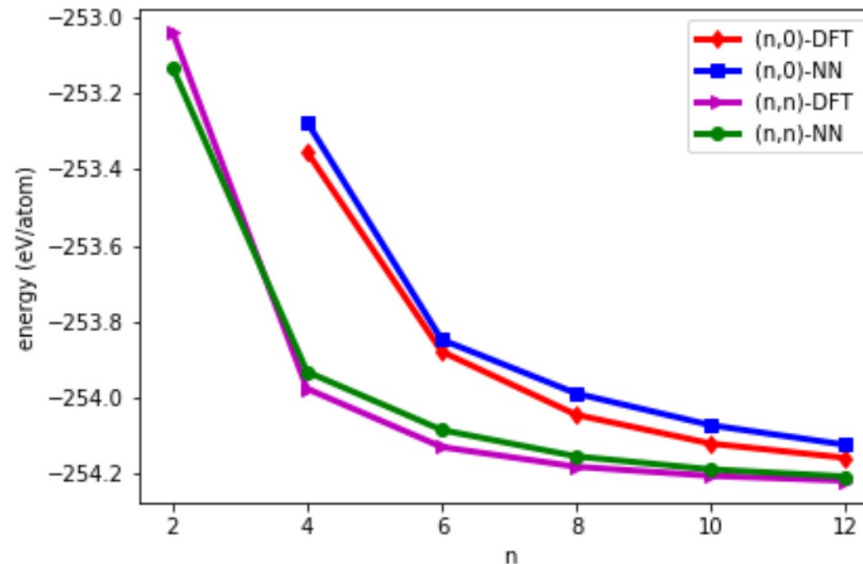
- configurations generated potential via NVT MD in which the system was heated up from 300 K to 1000K using Nose-Hoover thermostat chain over a period of 1ns.
- Excellent agreement with DFT





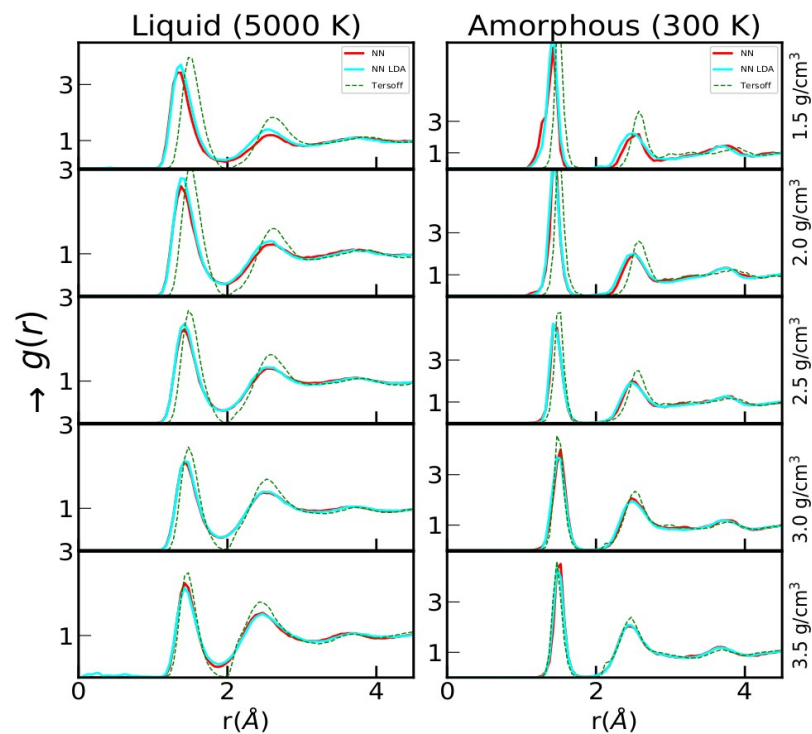
# Carbon Nanotubes

- Zigzag nanotube designated by  $(n,0)$  and Armchair nanotube designated by  $(n,n)$ .  $n$  specifies the diameter of the tube as
$$d(n, m) = \frac{a}{\pi} \sqrt{n^2 + nm + m^2}$$
,  $a$  is the lattice parameter
- Trends excellently captured
- Good agreement with DFT

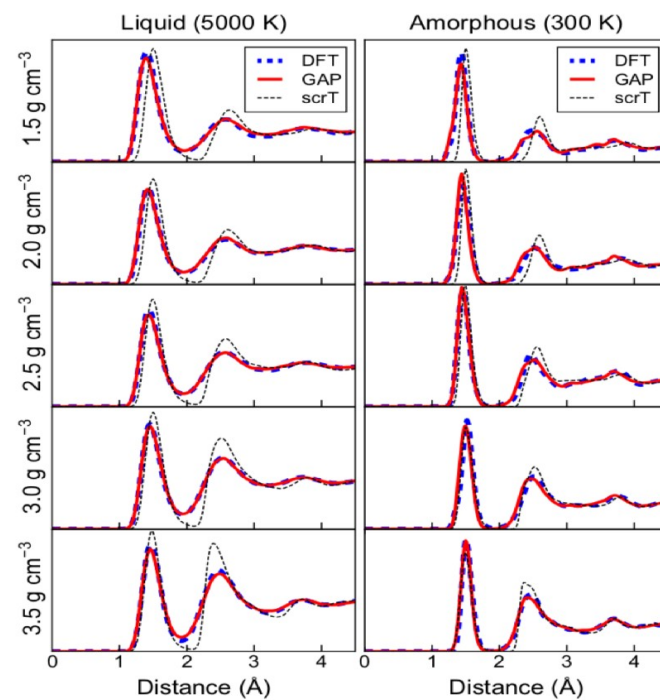


## Amorphous Carbon: radial distribution function

### a) Our result

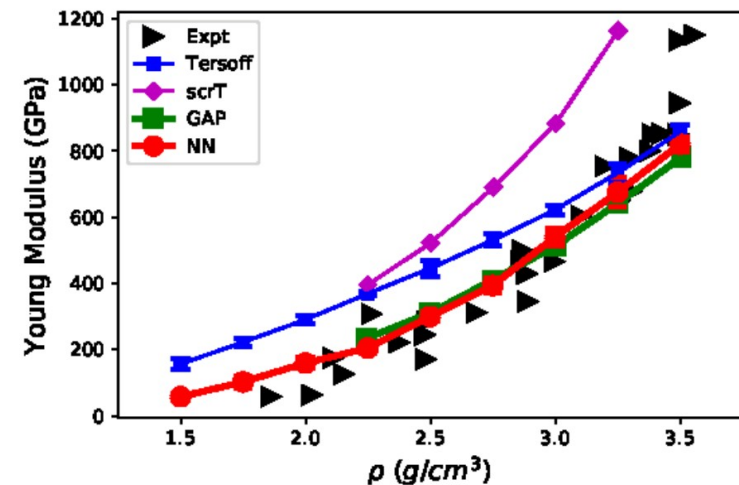
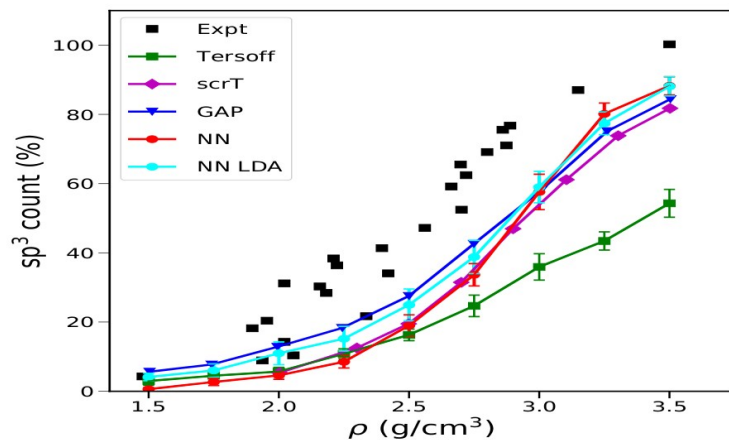


### b) GAP



V.L. Deringer and G.Csányi, PRB 95, 094203, (2017)

## Amorphous Carbon: $sp^3$ fraction and Young Modulus

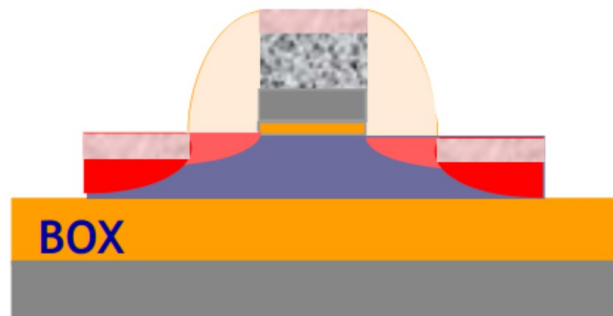


- Fallon et al. PRB 48, 4777 (1993).
- J. Schwan et al. Journal of Applied Physics 79, 1416 (1996)
- V.L. Deringer and G.Csányi, PRB 95, 094203, (2017)

- B.Schultrich et al. Diamond and Related Materials 5 (1996) 914-918
- B.Schultrich et al. Surface and Coatings Technology 98 (1998) 1097-1101

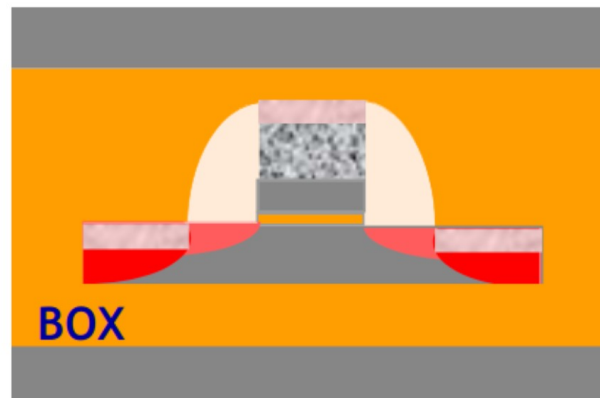
# Solid Phase Epitaxy for Silicon

Bottom transistor



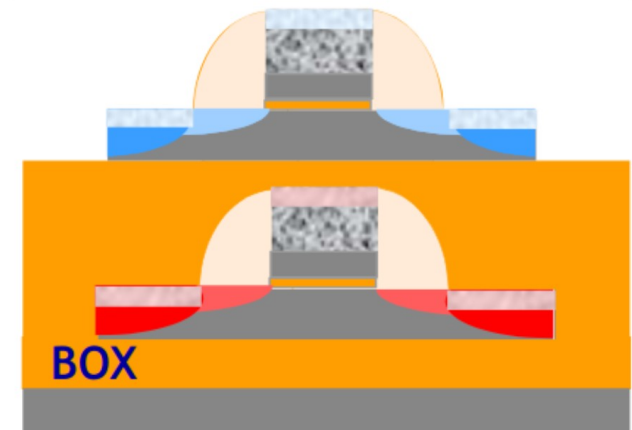
⚡ Salicide stability with top FET TB

Top film realization



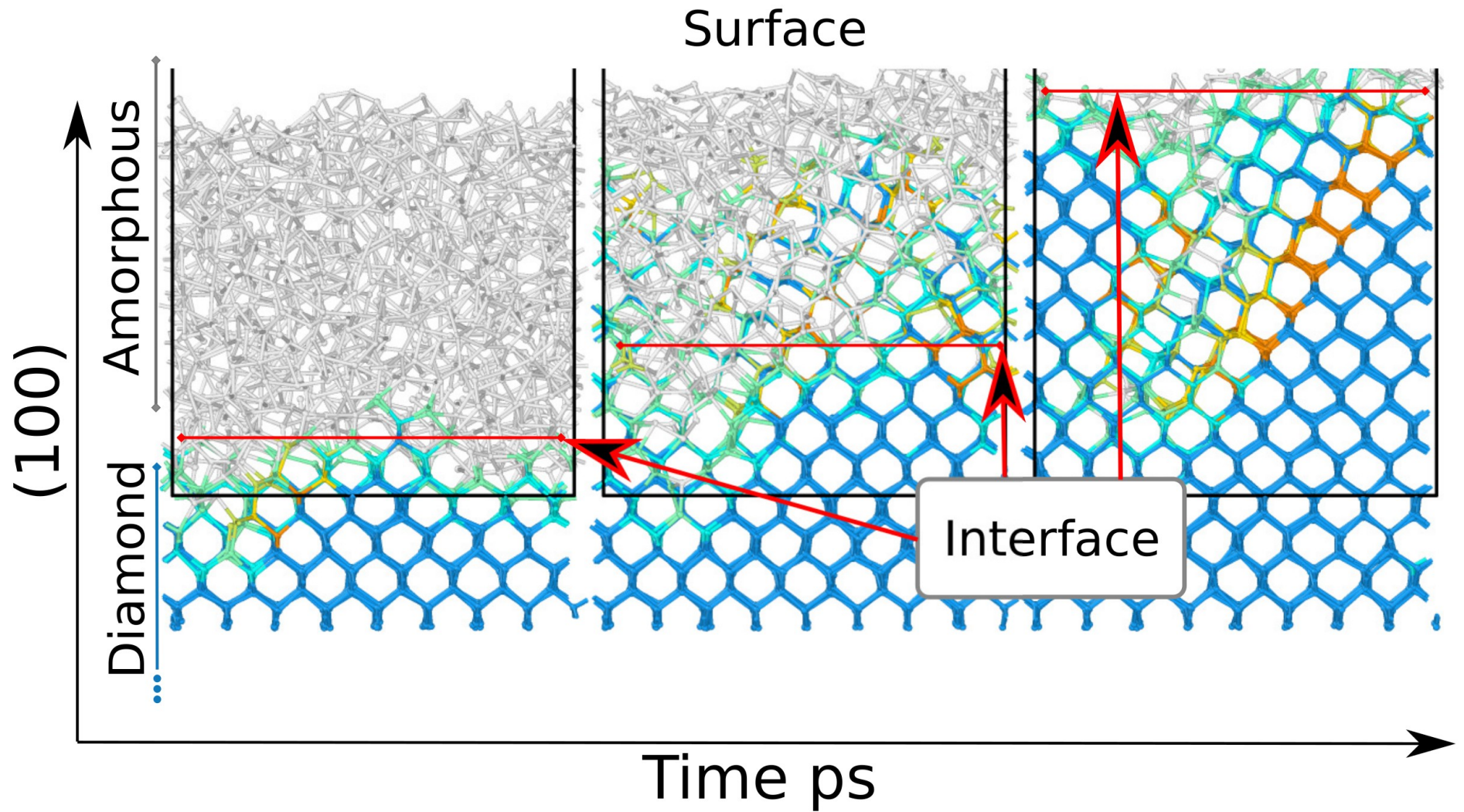
⚡ Cristalline quality/ thickness control

Top transistor



⚡ Reach high perf. with 650°C TB

# Problem statement



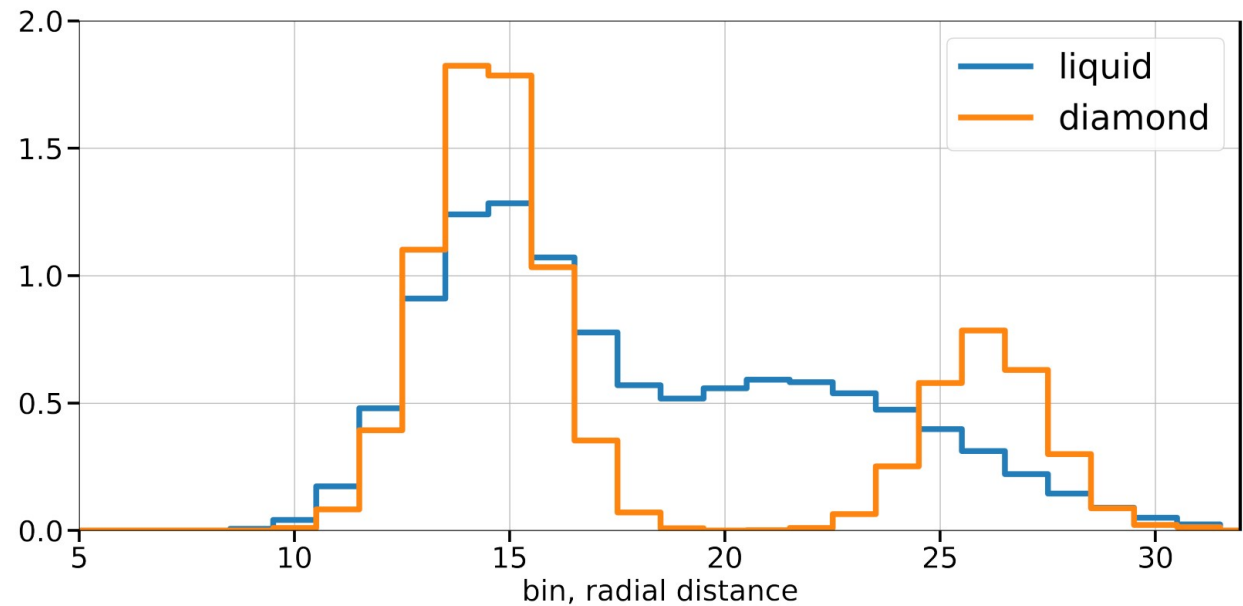
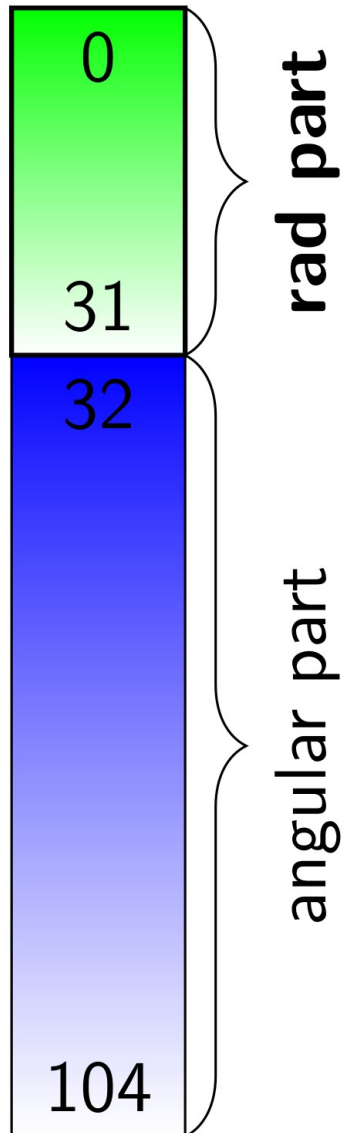
Olson and Roth 1988



The input:  $\mathbf{G}_i(\{\mathbf{x}_j\} | d(\mathbf{x}_i, \mathbf{x}_j) < r_{cut})$

The radial part

$$G_{m,s;i}^R = \sum_{\substack{\text{All atoms kind s} \\ i \neq j}} e^{-\eta(r_{ij} - R_m)^2} f_c(r_{ij})$$

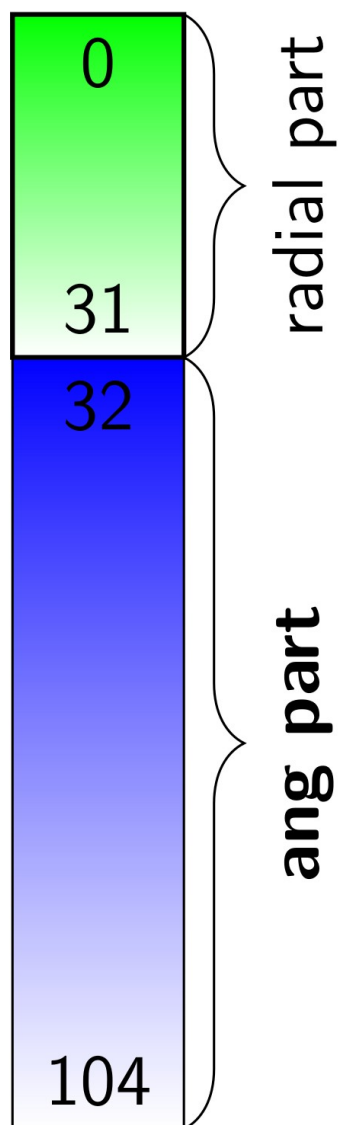


with thermal vibrations

Behler and Parrinello 2007



# The input: Descriptor

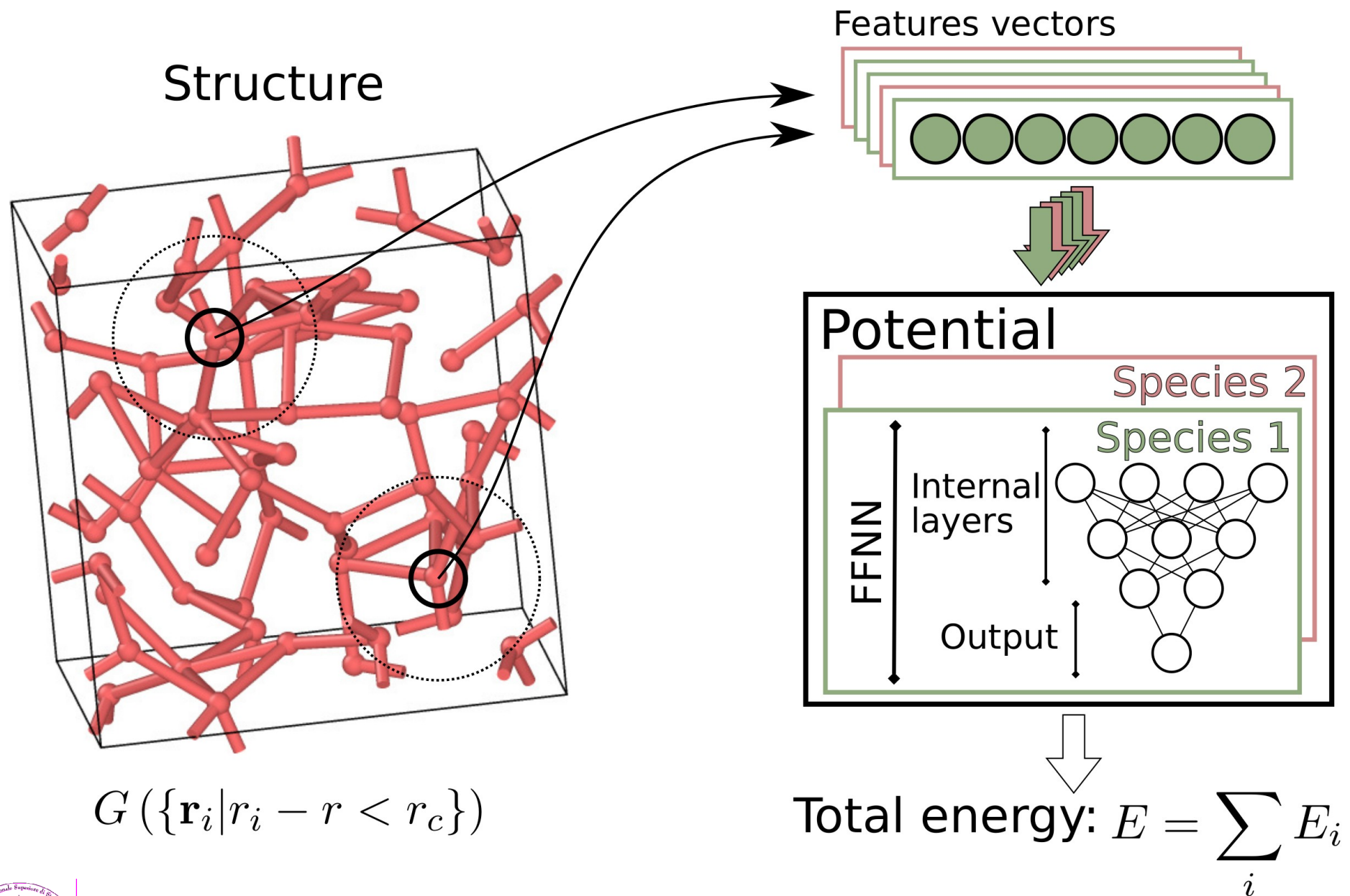


The angular part

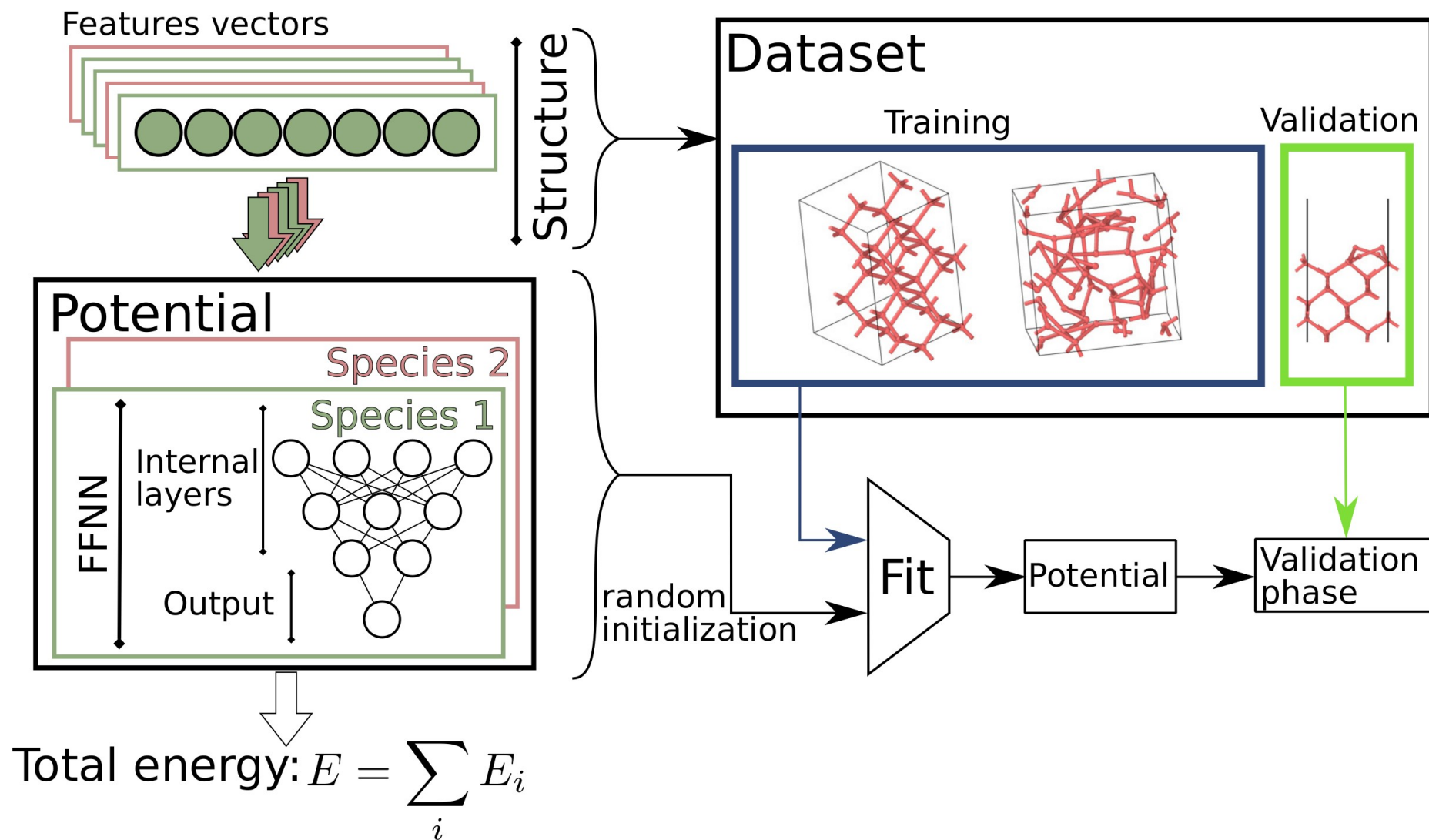
$$G_{n,m,s;i}^A = 2^{1-\xi} \sum_{j,k \neq i}^{\text{All atom of kind s}} (1 + \cos(\Theta_{ijk} - \Theta_n))^\xi e^{-\eta \left( \frac{r_{ij} + r_{ik}}{2} - R_m \right)^2} f_c(r_{ij}) f_c(r_{ik})$$

Lot et al. 2020; Smith, Isayev, and Roitberg 2017

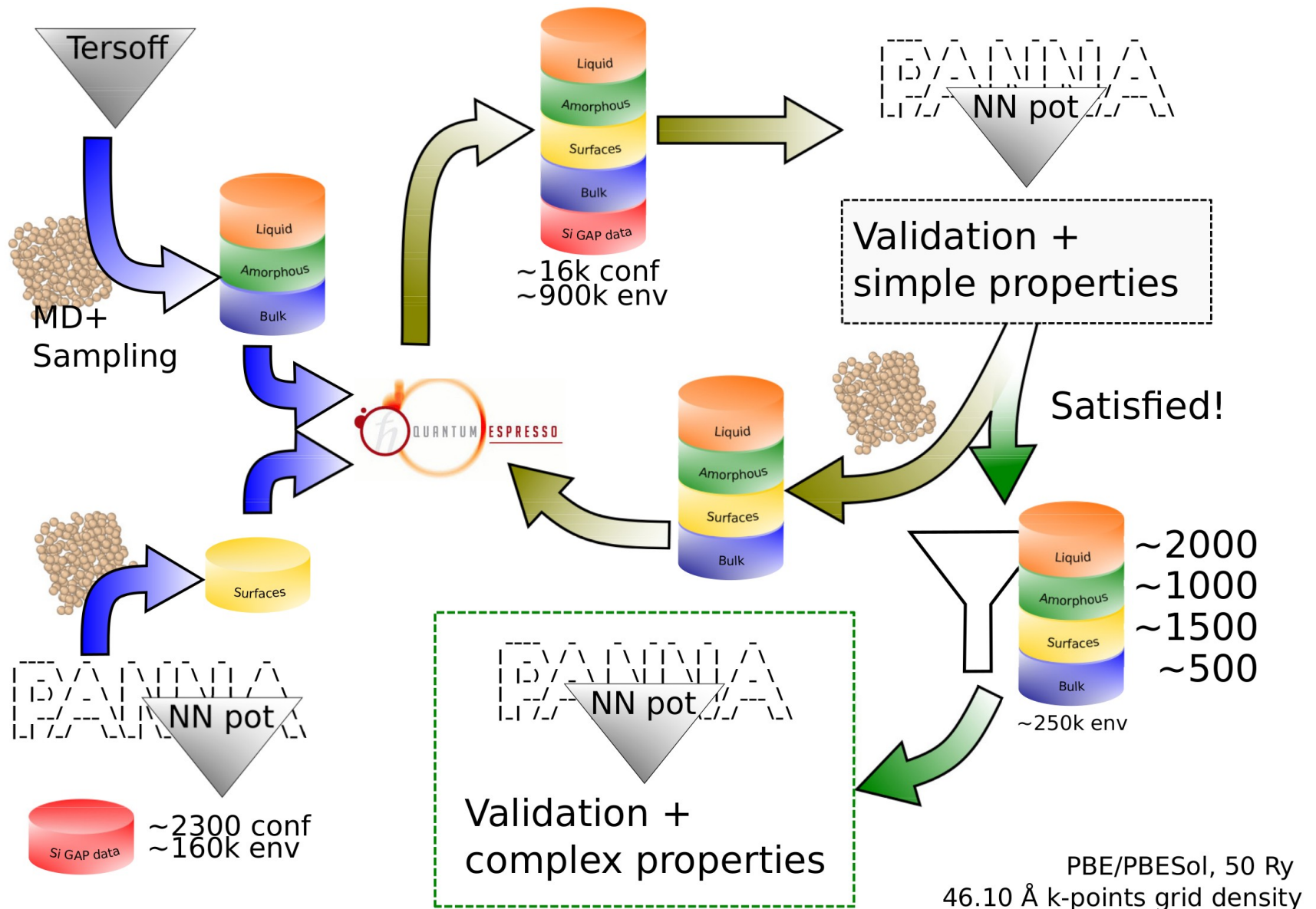
# From a FFNN to a potential



# The fitting phase

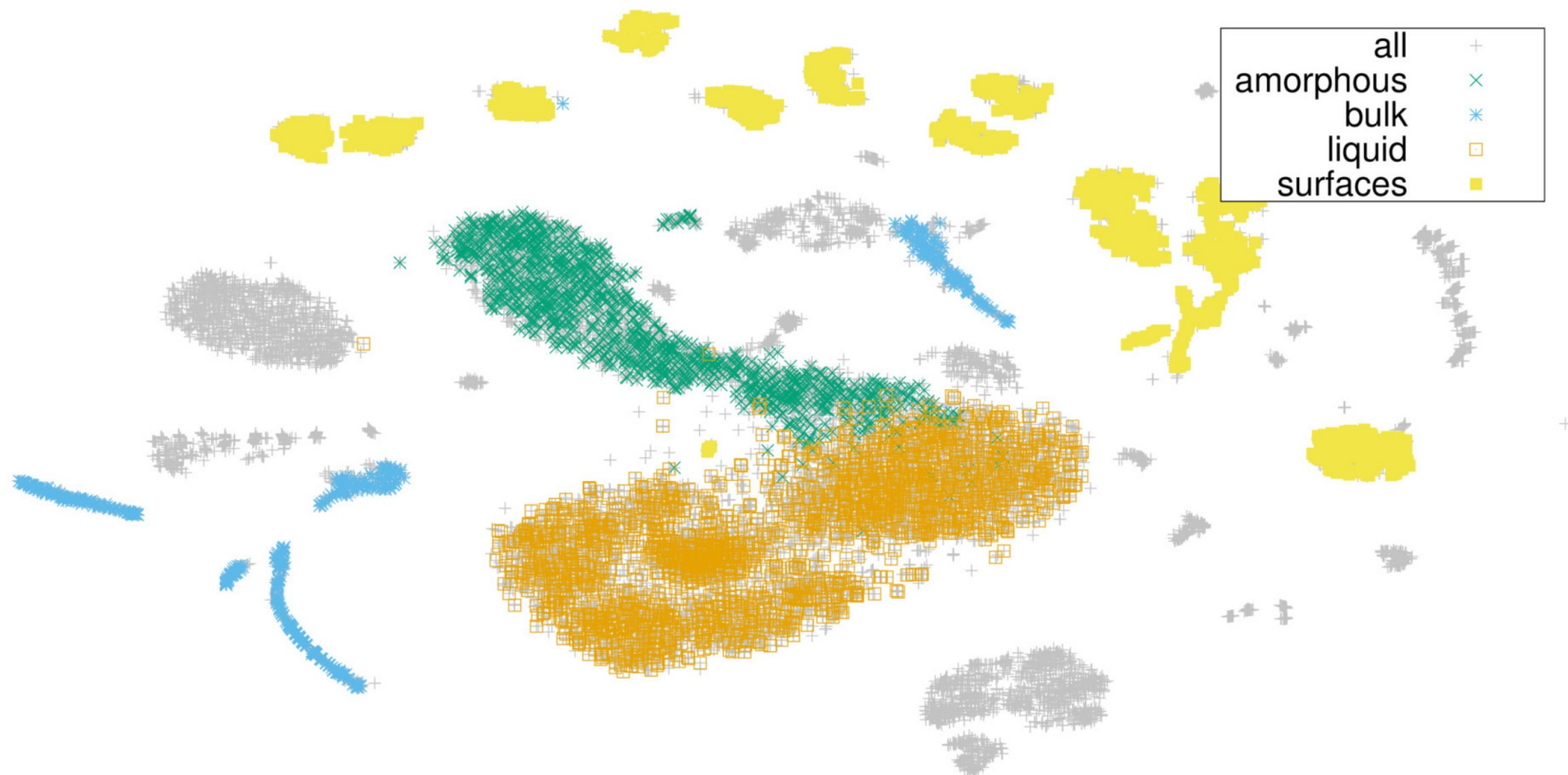


# Work workflow



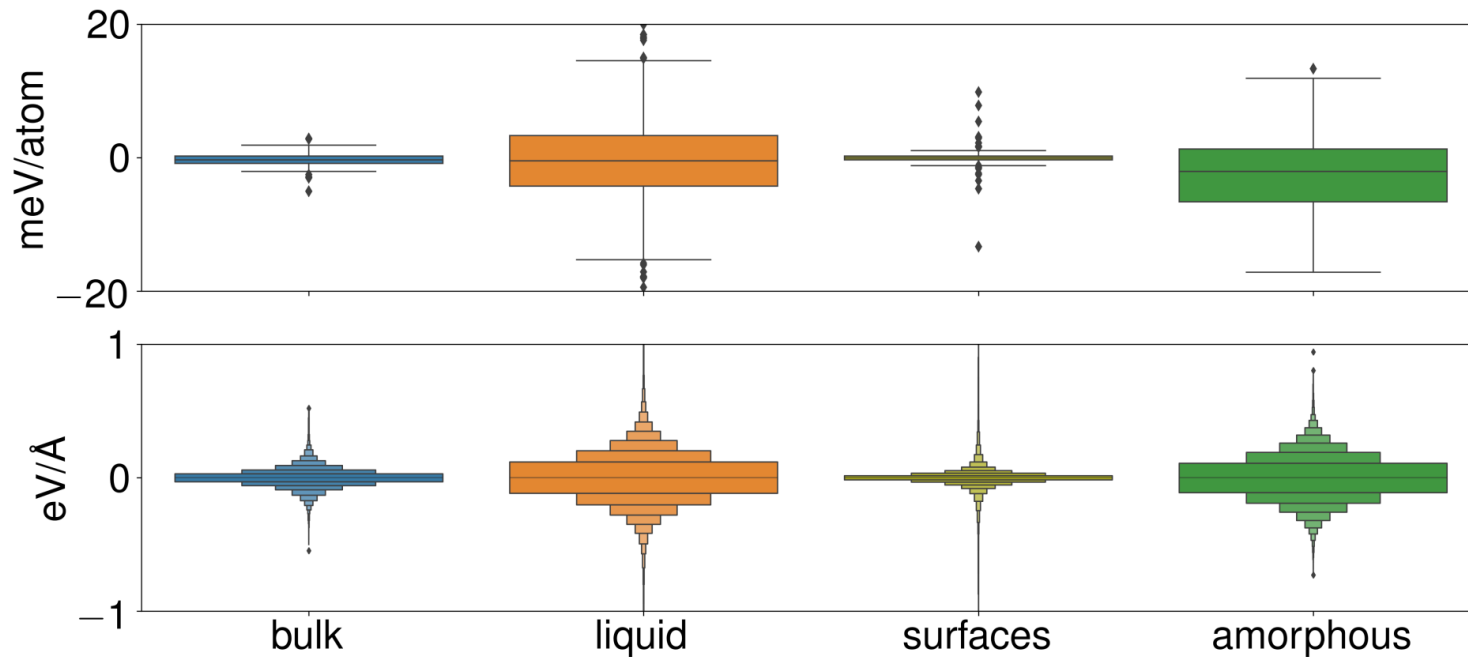


# Dataset and validation



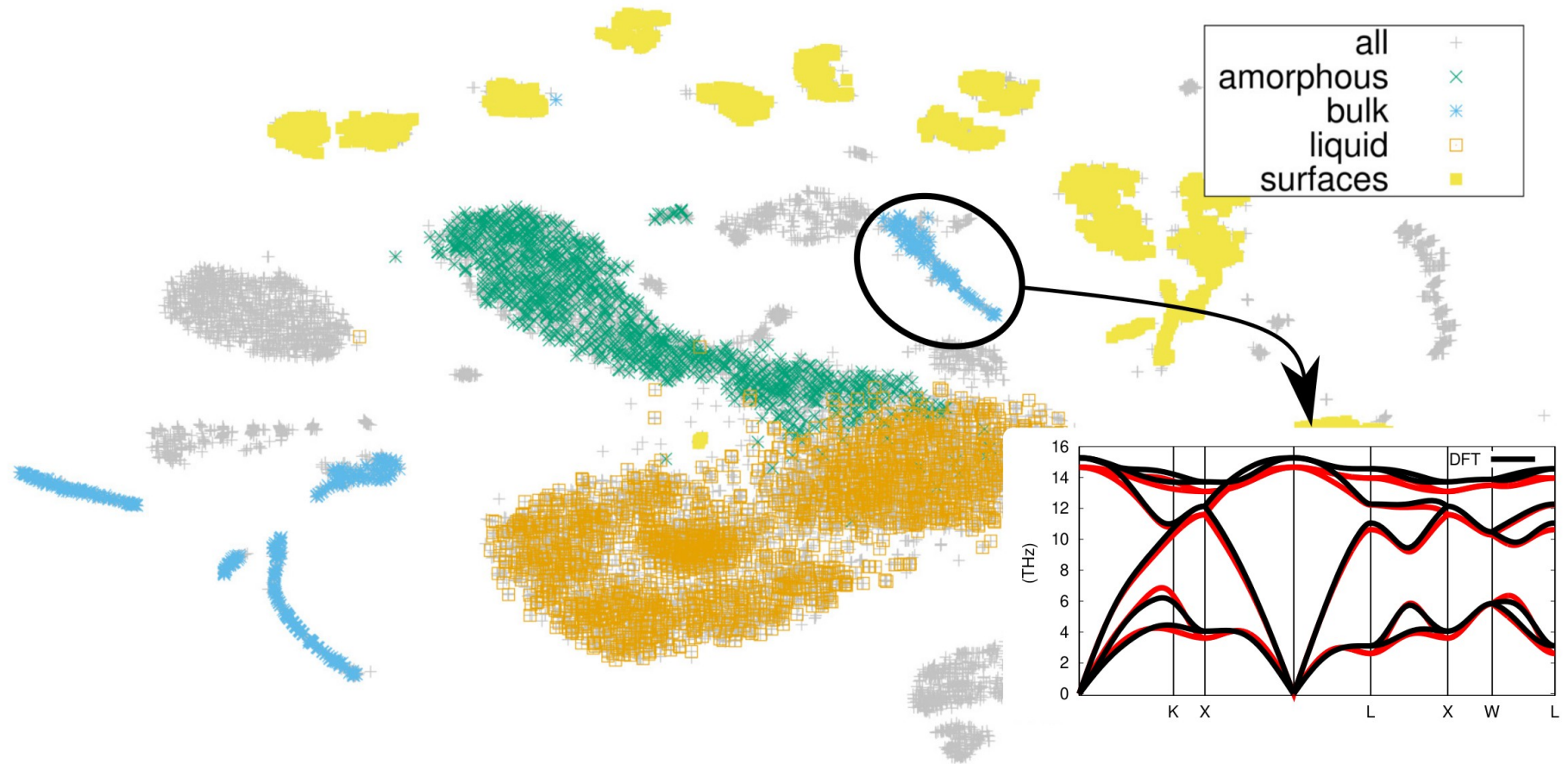
t-sne,  $\approx 5000$  points for  $\approx 250k$  environments

# Validation on the dataset

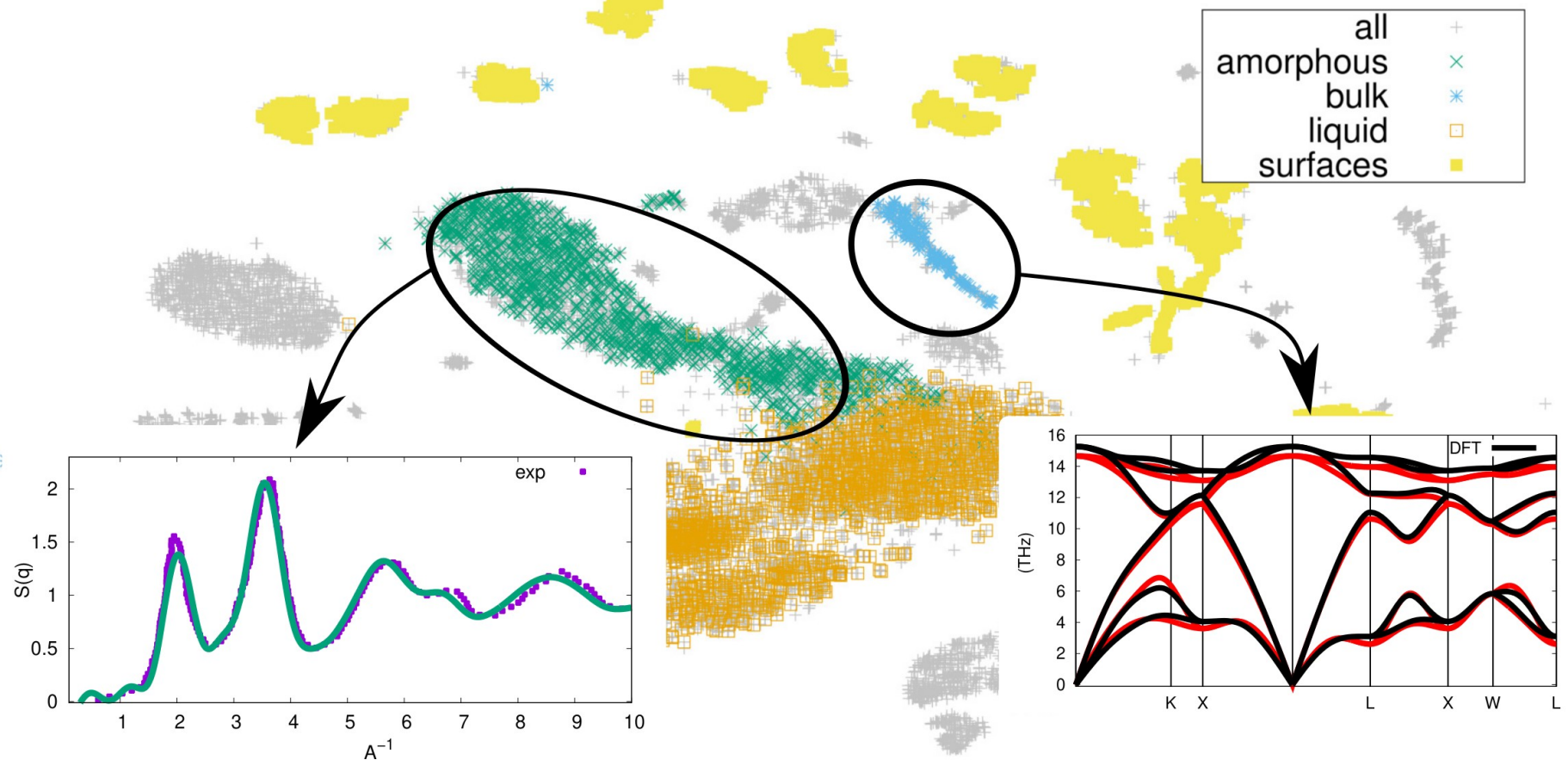


|                   | bulk | liquid | surfaces | amorphous |
|-------------------|------|--------|----------|-----------|
| Energy [meV/atom] | 0.9  | 7.5    | 3.4      | 5.8       |
| Forces [meV/Å]    | 66   | 196    | 103      | 170       |

# Validation on physical properties

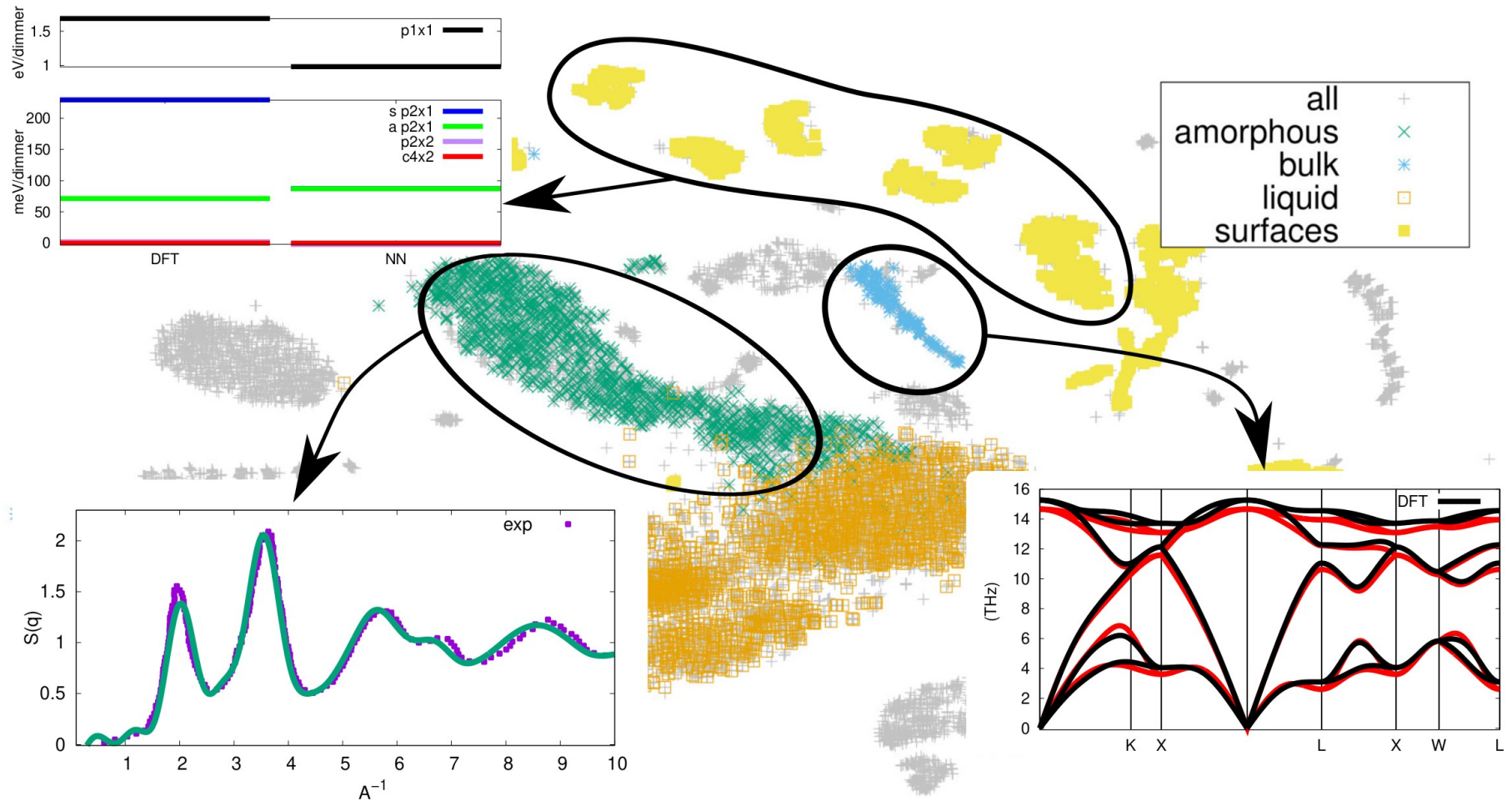


# Validation on physical properties



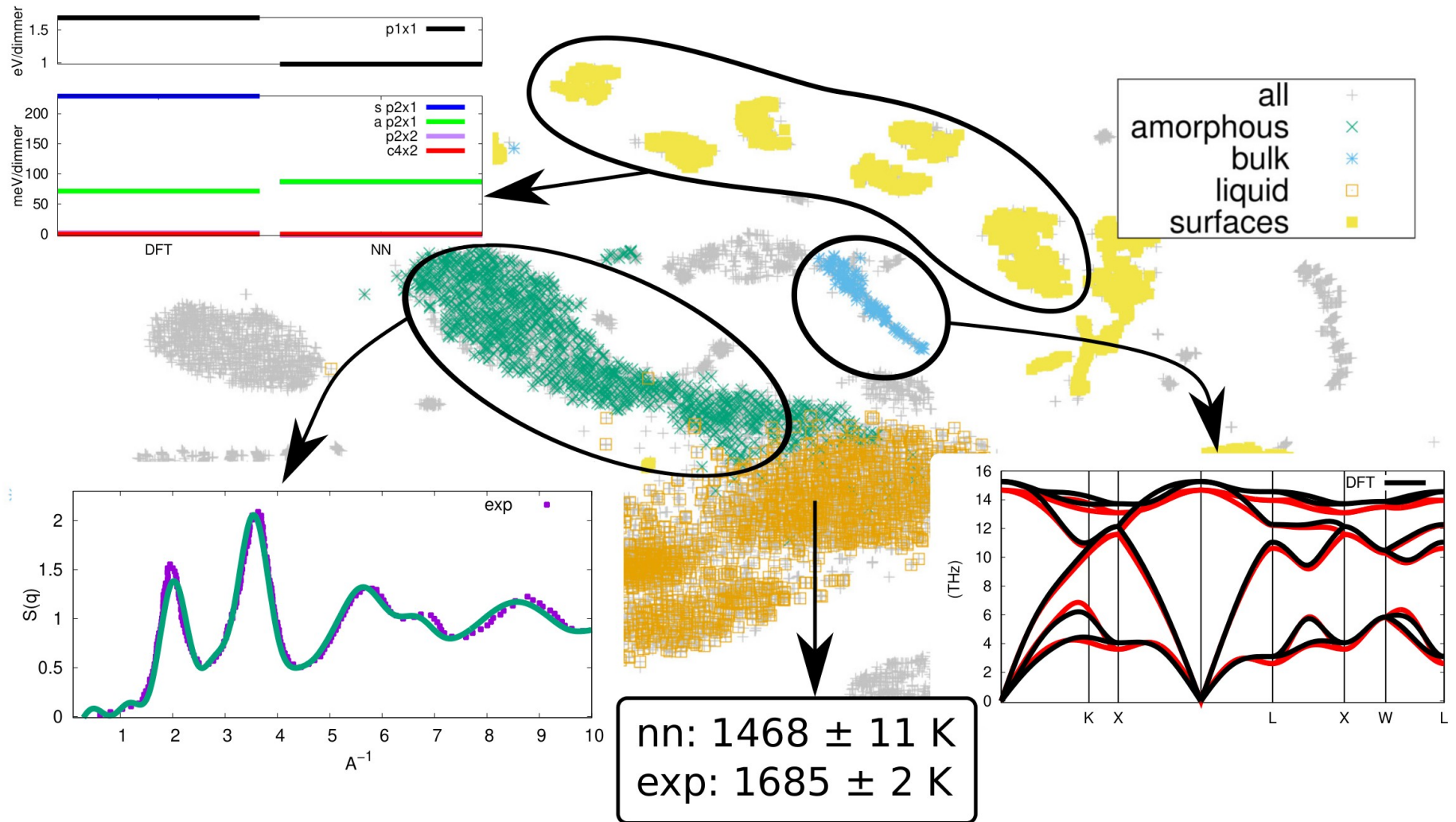


# Validation on physical properties



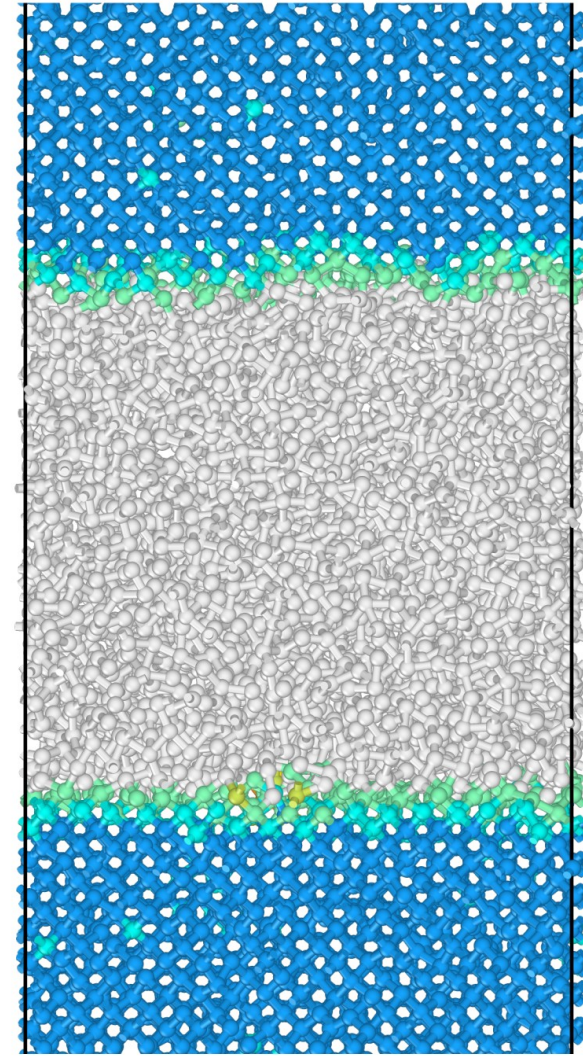


# Validation on physical properties



# Melting temperature

|             |                       |
|-------------|-----------------------|
| NN pbe      | $1468 \pm 11\text{K}$ |
| DFT pbe     | $1540 \pm 50\text{K}$ |
| NN PBESol   | $1194 \pm 28\text{K}$ |
| GAP PBESol  | $1213 \pm 21\text{K}$ |
| Experiments | $1685 \pm 2\text{K}$  |

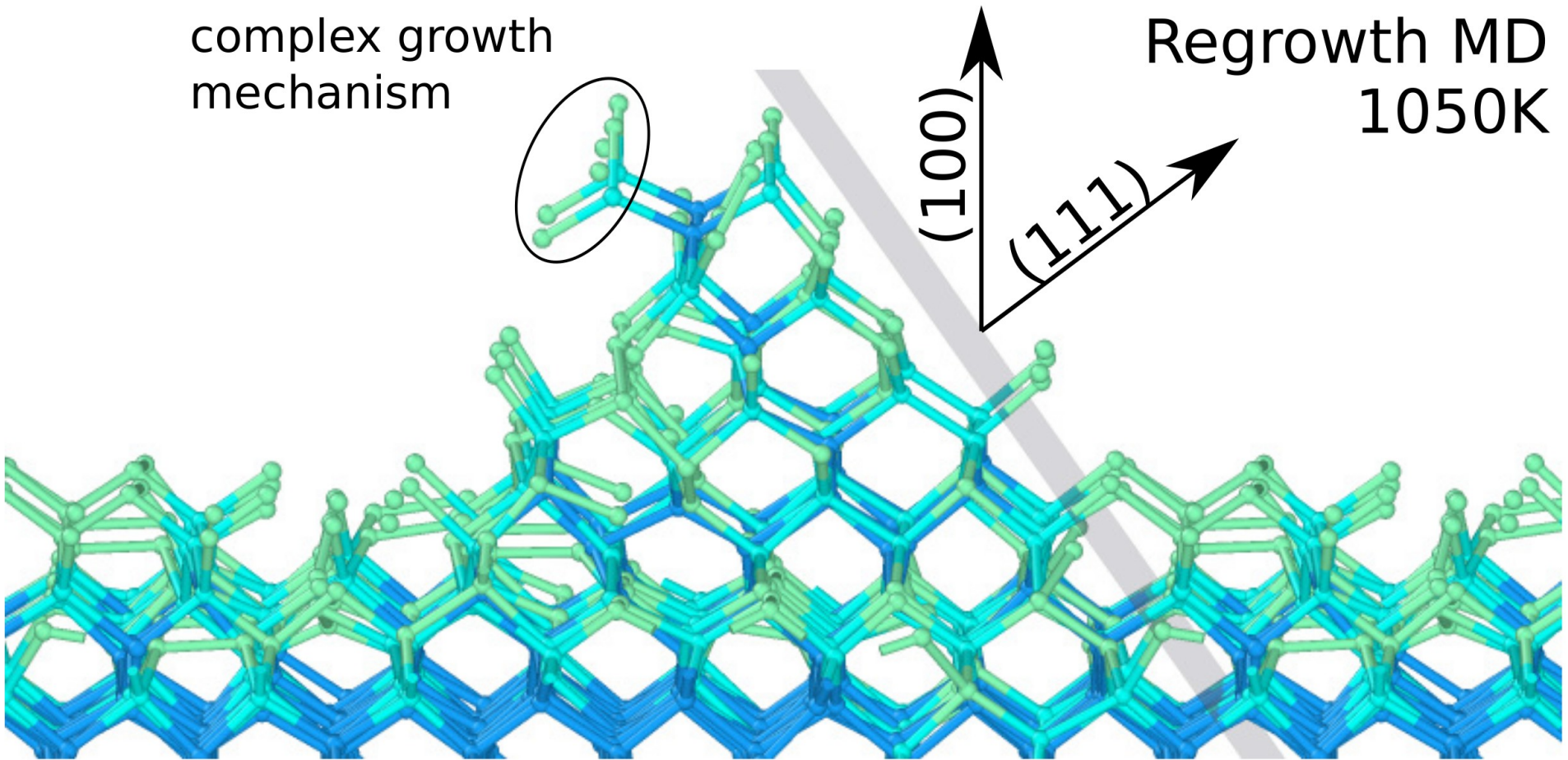


Yoo, Xantheas, and Zeng 2009; Jinnouchi, Karsai, and Kresse 2019

# SPE, What do we see?

complex growth  
mechanism

Regrowth MD  
1050K

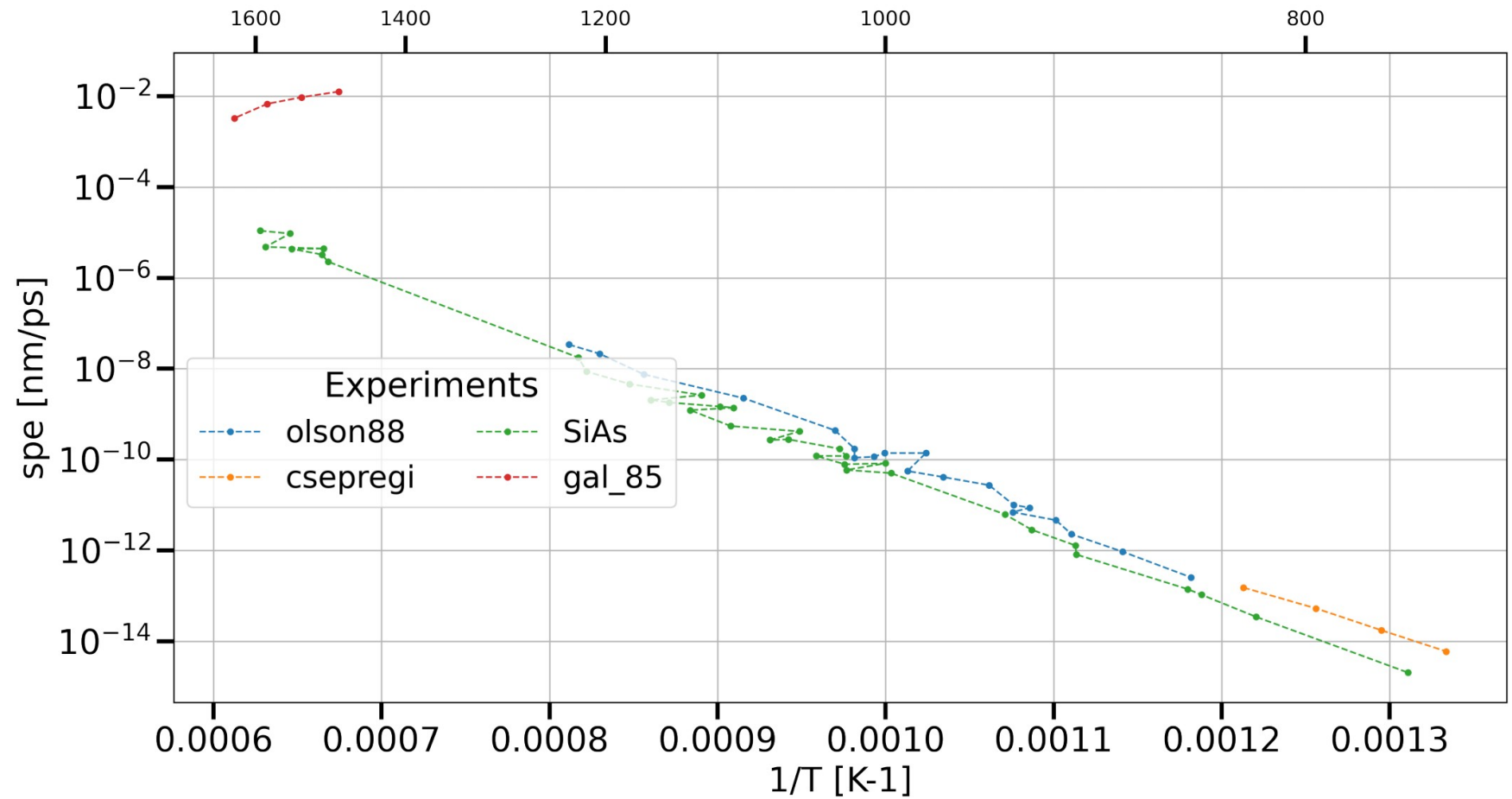


Thermally activated process:

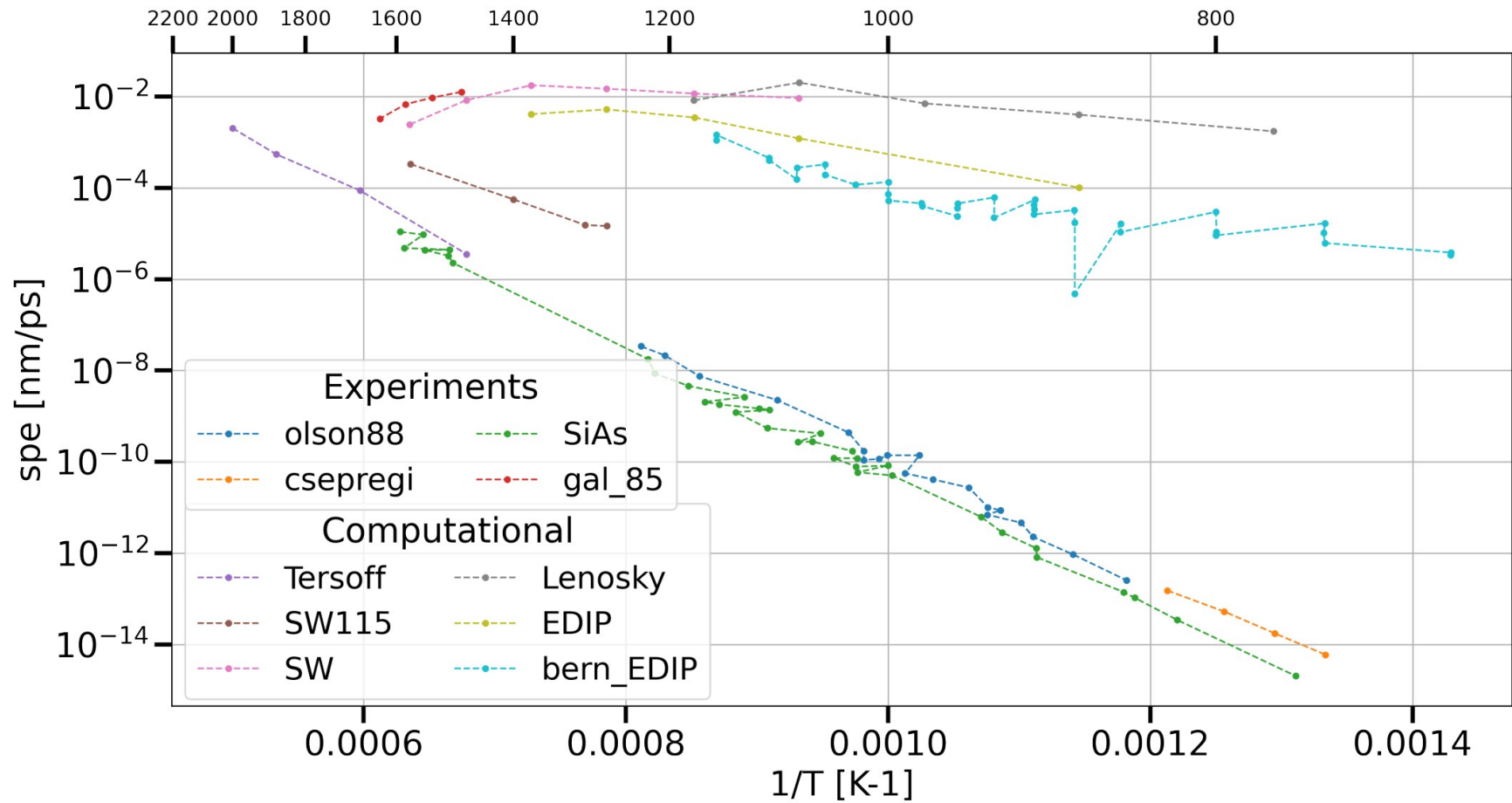
$$v = v_0 \exp\left(-\frac{\Delta E}{k_b T}\right)$$



# SPE, What do we see?

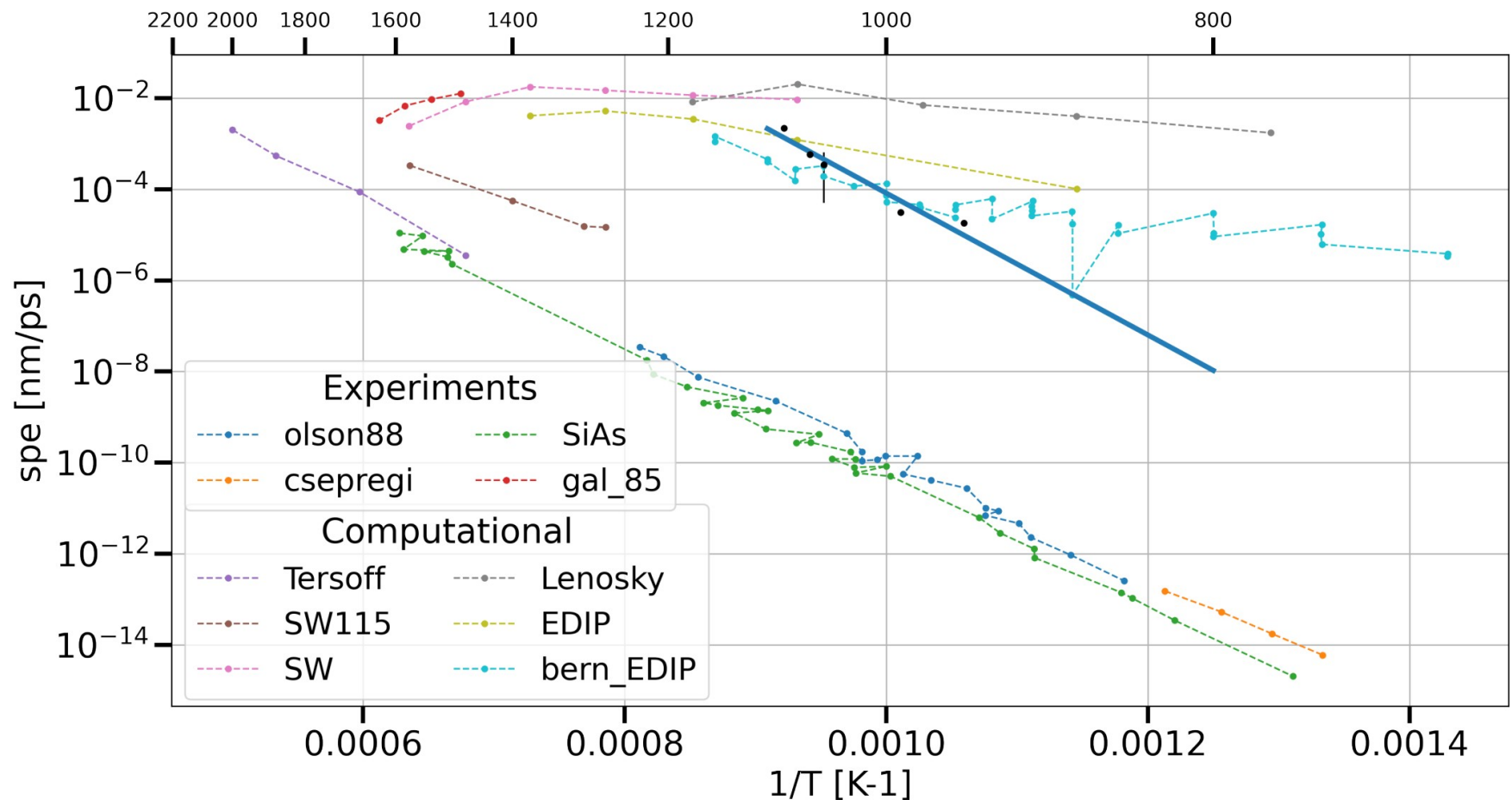


# SPE, What do we see?





# SPE, What do we see?



panna: 3.15 eV, experiments<sup>1</sup>: 2.73 eV



Olson and Roth 1988.

# Conclusion and outlook

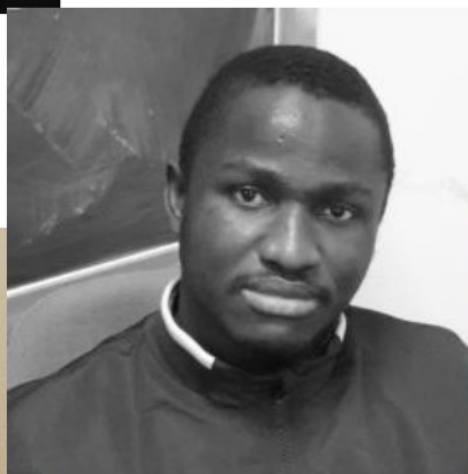
- NN potentials are a valid way to model physical phenomena at the atomistic level
- As a byproduct, PBE-sol xc-functional is not suitable to study thermal related phenomena in silicon
- We are obtaining a correct energy barrier for SPE with pure ab-initio data.
- Improve the amorphous quality
- Isolate the main events for SPE
- Develop a better KMC model.



Emine Kucukbenli



Ruggero Lot



Yusuf Shaidu



Franco Pellegrini



Stefano de Gironcoli